Swedish Dental Journal Supplement 222, 2012

Enamel of Primary Teeth

- morphological and chemical aspects

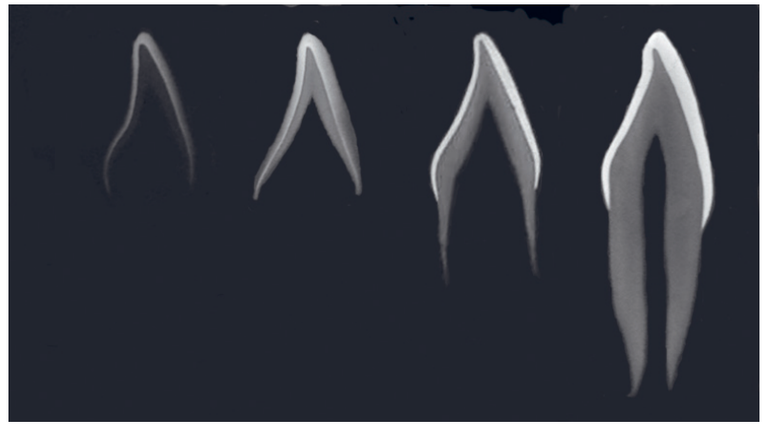

Nina Sabel

Institute of Odontology
at Sahlgrenska Academy
University of Gothenburg

UNIVERSITY OF GOTHENBURG

Nina Sabel Enamel of Primary Teeth - morphological and chemical aspects

The Sahlgrenska Academy

2012

ISBN 978-91-628-8361-4
Printed by Ale Tryckteam AB, Bohus

Enamel of Primary Teeth - morphological and chemical aspects

Nina Sabel

Department of Pediatric Dentistry
Institute of Odontology
Sahlgrenska Academy at University of Gothenburg

UNIVERSITY OF GOTHENBURG

Gothenburg 2012

Cover illustration: Microradiographs of tooth buds from individuals at 1, 2, 6 and 19 months of age.

Enamel of Primary Teeth - morphological and chemical aspects

nina.sabel@vgregion.se

Printed by Ale Tryckteam, Göteborg, Sweden 2012

Swedish Dental Journal Supplement 222, 2012
ISSN: 0348-6672
ISBN 978-91-628-8361-4
GUPEA http://hdl.handle.net/2077/28004

Enamel of Primary Teeth - morphological and chemical aspects

Nina Sabel

Department of Pediatric Dentistry, Institute of Odontology
Sahlgrenska Academy at University of Gothenburg
Göteborg, Sweden

ABSTRACT

Enamel is one of the most important structures of the tooth, both from a functional and esthetic point of view. Primary enamel carries registered information regarding metabolic and physiological events that occurred during the period around birth and the first year of life. Detailed knowledge of normal development and the structure of enamel is important for the assessment of mineralization defects. The aim of the thesis is to add more detailed information regarding the structure of primary enamel. The structural appearance of the neonatal line and the quantitative developmental enamel defect, enamel hypoplasia, was thoroughly investigated with a polarized light microscope, microradiography and scanning electron microscope. X-ray microanalysis of some elements was also performed across the enamel and the neonatal line. Postnatal mineralization of enamel at different ages and from different individuals was studied regarding the chemical content, by using secondary ion mass spectrometry. The enamel's response to demineralization was investigated in relation to the individual chemical content and the degree of mineralization of the enamel, by using polarized light microscope, microradiography, scanning electron microscope and X-ray microanalysis. The neonatal line is a hypomineralized structure seen as a step-like rupture in the enamel matrix. The neonatal line is due to disturbances in the enamel secretion stage. The enamel prisms in the postnatal enamel appeared to be smaller than the prenatal prisms. The hypoplasias showed a rough surface at the base and no aprismatic surface layer was seen in the defect. The enamel of the rounded border of hypoplasia appeared to be hypomineralized, with the bent prisms not being densely packed. Mineralization of enamel is a gradual process, still continuous at 6 months postnatally in the primary mandibular incisors. The thickness of the buccal enamel is reached at 3-4 months of age. Demineralization of enamel depends on the degree of mineralization and the chemical content of the enamel exposed. In a more porous enamel, deeper lesions will develop. The posteruptive maturation has a beneficial effect on the enamel's resistance to demineralization.

Keywords: Demineralization, enamel, enamel hypoplasia, microradiography, mineralization, neonatal line, polarized light microscopy, scanning electron microscopy, secondary ions mass spectrometry, X-ray microanalysis.

Swedish Dental Journal Supplement 222, 2012
ISSN: 0348-6672
ISBN: 978-91-628-8361-4
GUPEA http://hdl.handle.net/2077/28004

LIST OF PAPERS

This thesis is based on the following studies referred to in the text by their Roman numerals (*I-IV*).

I. Sabel N., Johansson C., Kuhnisch J., Robertson A., Steiniger F., Norén J.G., Klingberg G., Nietzsche S. Neonatal lines in the enamel of primary teeth - a morphological and scanning electron microscopic investigation.
Archieves of Oral Biology 2008; 53: 954-63.

II. Sabel N., Klingberg G., Nietzsche S., Robertson A., Odelius H., Norén J.G. Analysis of some elements in primary enamel during postnatal mineralization.
Swedish Dental Journal 2009; 33: 85-95.

III. Sabel N., Klingberg G., Dietz W., Nietzsche S., Norén J.G. Polarized light and scanning electron microscopic investigation of enamel hypoplasia in primary teeth.
International Journal of Paediatric Dentistry 2010; 20: 31-6.

IV. Sabel N., Robertson A., Nietzsche S., Norén J.G. Demineralization of enamel in primary second molars related to properties of the enamel.
Accepted for publication in The Scientic World Journal, 2011.

CONTENT

ABBREVIATIONS

EDJ	Enamel-Dentin-Junction
MRG	Microradiography
NNL	Neonatal line
POLMI	Polarized light microscopy
RI	Refractive Index
SEM	Scanning Electron microscopy
SIMS	Secondary Ion Mass Spectrometry
XRMA	X-ray microanalysis

1 INTRODUCTION

Enamel is one of the most important structures of the tooth, both from a functional and esthetic point of view. Enamel is also unique in the recording of metabolical disturbances during the time of tooth formation, when studied histologically. Primary enamel carries registered information regarding certain metabolical and physiological events occurring during the period around birth and the first year of life. Detailed knowledge of normal development and of the structure of enamel is important when assessing mineralization defects.

Teeth in the primary dentition start their mineralization during the gestational period and the last primary tooth is completed around 3–3.5 years of age ((Massler & Schour 1946; Lunt & Law 1974). Ameloblasts are highly differentiated and very specialized cells forming the enamel. They have limited capacity to recover from disturbances to their function and neither is enamel able to reform. Enamel is said to be a kymograph of the period of enamel formation. Therefore, histo-morphological studies of primary teeth may contain information of events affecting the ameloblasts during the prenatal and postnatal periods. The presence of a distinct incremental line (the neonatal line), related to the time of birth, makes it possible to distinguish between prenatally and postnatally formed enamel and also enables the dating of a disturbance.

Teeth, and especially enamel, undergo few or no morphological changes after the completion of mineralization and the eruption into the oral cavity. This is, in principle, also true for the chemical composition, with the exception of the enamel surface, which is highly reactive and subjected to changes related to, e.g., pH variations and fluoride exposition.

1.1 Normal and morphological aspects in enamel

Enamel is the outermost hard tissue of the tooth crown and is known to be the most highly mineralized tissue in the human body (Ten Cate

1994). Enamel consists of approximately 96% inorganic material, constituting biological hydroxyapatite crystals. Remnants of proteins from the period of development and water are also found in the enamel (Ten Cate 1994). The remaining components, by weight, are organic matter (ca 0.6%) and water (ca 3.5%) (Ehrlich *et al.* 2009).

Enamel has an inert cellular tissue and a thickness of approximately 1-2mm in permanent teeth and 0.5-1mm in primary teeth (Ten Cate 1994). The outer surface zone of enamel appears as a structure of prismless tissue, the aprismatic layer, in morphological analyses. The aprismatic layer is more frequently seen in primary teeth, where the width of the zone is larger compared to permanent teeth (Whittaker 1982). Of the teeth analyzed, more than 60% of the primary teeth had an aprismatic surface zone of 16-45μm thick, while half of the permanent teeth had an aprismatic zone of <5μm (Whittaker 1982).

Enamel is built of hydroxyl apatite crystals packed and arranged in prisms. The orientation of the crystals thus creates the appearance of prisms. The tightly aligned prisms extend from the dentin-enamel-junction to the enamel surface. The packing of crystals is slightly looser in the periphery of the prisms, the interprismatic space, compared to the intraprism structure. At macroscopic level, the packing of hydroxyl apatite crystals is very tight, though each crystal is separated by small intercrystalline spaces filled with water and organic material (Garnett & Dieppe 1990).

Genes, special conditions (such as hypocalcemia) and nutrition during the period of tooth development may influence the chemical content of the enamel (Aguirre *et al.* 1997; Aine *et al.* 1990; Nikiforuk & Fraser 1981). There are some elements, such as fluoride, that interfere with the normal processes of mineralization (Fejerskov *et al.* 1988). There are variations throughout the thickness of the enamel in the chemical and mineral content between primary and permanent enamel and between healthy individuals (Derise & Ritchey 1974; Sabel *et al.* 2009; Wong *et al.* 2004). The mineral content is shown to differ between the inner and outer enamel in the same tooth in sound enamel (Wong *et al.* 2004). Further, studies have indicated that the chemical content of enamel is depending on the occurrence of environmental trace elements (Lakomaa & Rytomaa 1977). Children born preterm have

different concentrations in the chemical content of the enamel compared to fullterm children (Rythén *et al.* 2010). The carbon concentration is found to be higher in children born preterm (Rythén *et al.* 2010).

Perikymata are seen as circular, horizontal bands around the tooth, frequently observed on the buccal surfaces in the clinic. Perikymata are the manifestations at the tooth surface of the Retzius lines. The Retzius lines are rhythmic incremental lines regularly spaced at 30-50μm in cross-sectioned enamel (Risnes 1990). The Retzius lines are a reflection of the bending of the prism during normal development (Gustafson 1959). Retzius lines can be seen in enamel with a polarized light microscope (POLMI), light microscope, scanning electron microscope (SEM) and in back-scattered images of scanning electron microscopy (BSE). In human enamel, the periodic emphasis is observed throughout the enamel as Retzius lines, occuring at approximately 8-10 days apart, and as cross-striations, once per day as a daily apposition of the prisms (Boyde 1997; Dean 1989). Cross-striations are an optical phenomena due to a change of the orientation of peripheral crystallites along the prisms (Helmcke *et al.* 1963).

Accentuated incremental lines are a result of various types of stress, due to physiological causes or pathological conditions (Gustafson 1959). The morphological appearance differs from the Retzius lines which are of a developmental origin (Gustafson 1959; Helmcke *et al.* 1963). The accentuated incremental lines are seen as step-like ruptures of prisms, interprismatic sheaths and/or the interprismatic spaces (Gustafson 1959). One of these normally found incremental lines is the neonatal line.

The neonatal line (NNL) is found in all primary teeth (enamel and dentin), and is described as a hypomineralized structure (Massler & Schour 1946). The NNL represents a growth pause in the enamel and is seen as a biological landmark of birth (Schour 1936). Enamel formed prior to the NNL, the enamel between the NNL and the enamel-dentin-junction (EDJ), is called prenatal enamel. Postnatal enamel represents the enamel between the NNL and the surface. Prenatal enamel appears to have a more homogenous structure compared to postnatally formed enamel (Massler & Schour 1946;

Norén *et al.* 1983). The location of the neonatal line differs in teeth due to tooth germs being at different developmental stages when children are born, thus the location of the NNL in the enamel is directly related to the gestational length (Szpringer-Nodzak 1984). A tooth at a later developmental stage at birth will have the NNL positioned more cervically (Szpringer-Nodzak 1984).

The neonatal line has previously been found to vary in thickness (Norén 1983; Norén 1984; Ranggard *et al.* 1995). In primary teeth from children of diabetic mothers, the NNL appears to be wider when examined in polarized light microscopy and by microradiography (Norén 1984). Also, children with a low gestational weight are shown to have a wider NNL compared to children with normal birth weight (Norén 1983).

The histological appearance of undecalcified enamel is well documented, however, its structure and composition are complex and more than one method of investigation is needed for studying enamel. POLMI investigations of enamel have shown that negatively birefringent enamel has a relatively homogenous structure, while positively birefringent enamel is relatively heterogeneous (Gustafson 1959). Additionally, POLMI investigations, in combination with microradiography, have shown that areas with negatively birefringent enamel appeared more radio-opaque and areas with positively birefringent enamel were radio-lucent. This indicates that negatively birefringent enamel contains more minerals than positively birefringent enamel (Gustafson 1959).

A single enamel prism is developed from one ameloblast (Skobe 2006). The prisms extend from the EDJ and continue toward the enamel surface (Fig. 1). The mean prism diameter of primary enamel is 2.9µm (±1.2µm) (Radlanski & Renz 2006). The angulations of the prisms toward the surface vary along the crown of the tooth, and are more perpendicular in the cervical area compared to approximately 70° in the coronal area (Radlanski & Renz 2006).

The crystal orientation in the prisms is well organized. The prism is principally formed like a cylinder (cross-sectioned formed like a keyhole) and the crystals forming the prism are parallel to the prism's

long-axis. This is valid for the most central crystals; the crystals in the periphery of the prisms are inclined to an increasing degree the further away they are from the prism center (Ten Cate 1994). Each prism is surrounded by the interprismatic space, where crystals are orientated in different directions (Ten Cate 1994). This is significantly and clearly seen in ¾ of the cross-sectioned prism (Ten Cate 1994). The interprismatic space is larger in hypomineralized enamel, where the diameter of prisms is smaller (Fig. 1) (Fejerskov *et al.* 1975).

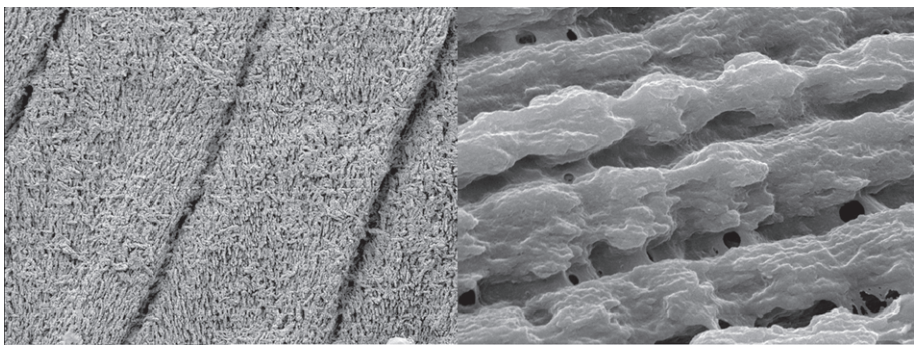

Figure 1. SEM images of normal enamel (left) and hypomineralized enamel (right). (Magnification 5 000x.)

The chemical content of enamel is fairly equally distributed in normal enamel in healthy individuals, even though individual variations in the chemical content and the degree of mineralization of enamel are seen (Hallsworth *et al.* 1972; Hallsworth *et al.* 1973; Lodding 1981; Norén *et al.* 1983; Sabel *et al.* 2009; Wong *et al.* 2004). The hydroxyl apatite in human enamel is not an exact compound since biological mineralization is influenced by trace elements in the environment during enamel formation (Lakomaa & Rytomaa 1977).

1.2 Developmental defects

Macroscopically, dental enamel normally has an even shade of translucent whitish color and a glossy smooth surface, however, in the clinic, defects in enamel are frequently seen. Developmental defects of enamel are deviations from the enamel's normal appearance,

originating from enamel organ dysfunction (Clarkson 1989). The classification of the defects is based on the clinical macroscopic appearance. The main three types of defects are demarcated opacity, diffuse opacity and enamel hypoplasia (Clarkson 1989). An opacity is a qualitative defect reflecting a hypomineralization of the enamel. Whereas enamel hypoplasia is a quantitative defect.

Developmental disturbances in enamel are seen in both the primary and permanent dentitions and may have a number of different etiological backgrounds, some being chronological, i.e., may be related to a specific time or period during enamel formation.

1.2.1 Hypomineralization of the enamel

During the maturation stage, matrix proteins are resorbed. If the matrix remains, the proteins exert an inhibitory effect and cause the enamel to incompletely mineralize (Robinson *et al.* 1989). This is denoted enamel hypomineralization and may occur locally on a single tooth or affect all teeth in a dentition. The degree of enamel hypomineralization may differ and may have different types of boundaries in normal enamel (demarcated or diffuse). Enamel hypomineralization may clinically be seen as a white, yellow and/or brown opaque region on a tooth, an area being less mineralized than normal enamel. It is likely that protein (albumin) from serum is an inhibitor of full mineralization in the calcium hydroxyapatite crystals (Garnett & Dieppe 1990; Robinson *et al.* 1992). Albumin might enter the enamel organ during the maturation stage by extravasation, causing visible white/opaque and less mineralized areas on the tooth surface (Robinson *et al.* 1992).

Fluoride is an important element during the mineralization of dental hard tissues and increases the lattice stability of the fluoridated apatite crystallites, however, it can also significantly alter the mineralized tissue. Fluoride is a well-known factor contributing to developmental disturbances in the enamel. When systemically administrated in excessive amounts during tooth mineralization, the enamel may become hypomineralized, a condition called dental fluorosis (Fig. 1) (Fejerskov *et al.* 1988). Additionally, fluoride plays an important role in the post eruptive mineralization of enamel and for the prevention of

demineralization, when locally administrated to the tooth surface, making the fluoridate apatite less soluble in acid (Fejerskov *et al.* 1996).

1.2.2 Dental fluorosis

Dental fluorosis is a dose-dependent response of hypomineralization to fluoride exposure during tooth development (Fejerskov *et al.* 1988). The amount of fluoride intake is in direct proportion to the outcome of the mineralization disturbance (Fejerskov *et al.* 1988). During amelogenesis (secretion and/or maturation stage), fluoride inhibits normal mineralization taking place (Rozier & Dudney 1981). Exposure to excessive fluoride intake during the long-lasting period of tooth formation may lead to signs of dental fluorosis in the whole dentition (Fejerskov *et al.* 1988).

The enamel in teeth with dental fluorosis is more porous compared to normal enamel, making the appearance of low grade dental fluorosis appear white (Fejerskov *et al.* 1975). The porosities are located at the periphery of the prisms, reflecting the dysfunction of the final growth of the enamel crystals (Fig. 1) (Fejerskov *et al.* 1988). Therefore, the prisms are less densely aligned, contributing to enamel of a more porous nature, especially in the outer part (Fejerskov *et al.* 1988; Fejerskov *et al.* 1975). The severity of enamel with dental fluorosis is negatively correlated to the micro-hardness of the enamel; the more severe a dental fluorosis, the less resistance the enamel is to indentations (Vieira *et al.* 2005).

Hypomineralized enamel in fluorosis might be a result of the retention of amelogenin in the fluorosed enamel (Zhang *et al.* 2006). The effect of fluoride during enamel development has been shown to down-regulate a proteinase, which contributes to the retention of amelogenin in the enamel (Zhang *et al.* 2006).

1.2.3 Enamel hypoplasia

Enamel hypoplasia is a quantitative defect of enamel, resulting from an impact to the ameloblasts during the period of enamel formation (Fig. 2) (Hu *et al.* 2007; Suga 1989). It is a disruption of the enamel matrix secretion during the secretion stage (Hu *et al.* 2007). Hypoplasia etiology is based on hypocalcemia (Nikiforuk & Fraser 1981). Low serum values of calcium during the enamel formation have a dose-responsive relationship to hypoplasia in primary teeth (Nikiforuk & Fraser 1981; Ranggard & Noren 1994; Ranggard *et al.* 1995).

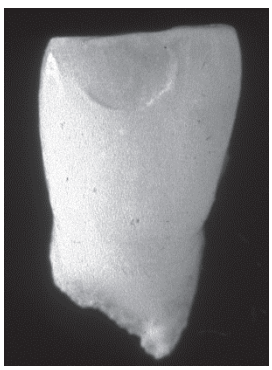

Figure 2. Enamel hypoplasia incisally located on the buccal surface on a mandibular incisor.

The greatest risk for developing hypoplasia and enamel developmental defects in the primary teeth is the period between birth to ten months of age (Massler & Schour 1946). Prenatally developed enamel hypoplasia is rare, but has been found in children of mothers malnourished or intoxicated during pregnancy (Massler & Schour 1946). Enamel hypoplasia in primary teeth is located corresponding to the NNL (Norén 1983). The hypoplasia has cervical round borders, formed by bent prisms in the enamel (Norén 1983).

Enamel hypoplasia in the primary second molar has been reported in 3.9% of a child population (Hong *et al.* 2009). In addition, hypoplasia was found in 20% of the teeth in the primary dentition (Needleman *et al.* 1991). Enamel hypoplasia is more likely to be seen in mono and dizygotic twins than in singletons births, with the most reasonable

cause being environmental factors, including intubation (Taji *et al.* 2011). Children with low birth weight and a short gestational age showed an increased prevalence of hypoplasias (Vello *et al.* 2010). Low birth weight was correlated to a higher prevalence of hypoplasia (56.9%) compared to children with normal weight (16%) (Vello *et al.* 2010). Children having a shorter gestational age showed more teeth (1.6) displaying hypoplasia compared with normal termed children with 0.3 affected teeth (Vello *et al.* 2010).

1.3 Development of enamel

The calcification of the primary dentition starts *in utero*. The sequence of the mandibular teeth starts with central incisors followed by the lateral incisors, canines, first molars and second molars (Kraus & Jordan 1965). The central and lateral incisors and the canines start their calcification at one point, as an individual growth center (Kraus & Jordan 1965). The neighboring ameloblasts at the calcification front successively begin their formation at later intervals (Kraus & Jordan 1965). The central incisors start calcification at 15 weeks of gestation and the lateral incisors start at 16 weeks of gestation (Kraus & Jordan 1965). The initial calcification of the canines is at 17 weeks of gestation (Kraus & Jordan 1965). The initiation of calcification of the second primary molar starts with the mesiobuccal cusp approximately 18-19 weeks *in utero* (4.5 lunar months) (Kraus & Jordan 1965). In the primary second molars, the calcification is initiated at the mesiobuccal cusp, followed by the mesiolingual, distobuccal and distolingual cusp (Kraus & Jordan 1965). At 36 weeks *in utero,* the cusps and the occlusal surface are covered by a calcified layer of enamel, though a considerable deposition of enamel is laid down before completion of calcification (Kraus & Jordan 1965).

The mineralization of enamel in the primary second molars is finished by the end of the first year of life (Lunt & Law 1974). Therefore, at nineteen months of age (Study *II*), the primary second mandibular incisor is considered to be fully developed according to schematic views of the chronology of developing primary teeth (Massler & Schour 1946).

In the initiation of enamel, the ameloblasts move from the EDJ. Dentine sialophosphor protein and tuftalin contribute to nucleation or mineral initiation (Robinson *et al.* 1998). Tuftalin acts as a precursor at the start of enamel formation at the EDJ, where tuftaline plays a role in the initial interaction between the mesenchymal and ectodermal cells, leading to dentin and enamel formation (Deutsch *et al.* 1998). After the first initial mineralization of the dentin, the ameloblasts are differentiated and start their secretion of the enamel matrix. The union of dentin and enamel is tight, since the enamel matrix meshes into the dentin (Boyde 1997). The enamel formation has biochemically and visibly definable stages (Robinson *et al.* 1981):

Secretion stage: Partially mineralized matrix is secreted. The enamel has a translucent appearance.

Transition stage: Replacement of degraded matrix by tissue fluid occurs. The enamel has a translucent appearance.

Maturation stage: Residual matrix is replaced by tissue fluid which is replaced by mineral uptake associated with crystal growth in width and thickness. The enamel has a white and porous (opaque) appearance.

One prism is formed by one ameloblast throughout the formation from the EDJ toward the surface (Skobe 2006). During the secretion stage, the matrix is secreted by the ameloblasts from two preferred sites (Boyde 1997). The superficial site forms the most prominent parts of the developing enamel surface and the second location is from the Tomes´ process (Boyde 1997). From the prominent location of the ameloblasts, the long crystals are perpendicular to the general plane of developing enamel (interpit material) (Boyde 1997). From the Tomes' process, the crystals have their c-axis along the prism orientation, nearly perpendicular to the enamel surface (Boyde 1997). The crystals grow almost parallel to each other, with the larger sides of the hexagonal cross-section aligned and clustered in groups (Boyde 1997). The elongation of the crystals during the secretion stage is dependent on the enamelin. Without enamelin, the initiation and elongation of the enamel crystallites appears to be absent (Hu *et al.* 2008). The different stages during enamel formation are guided and controlled by various

enzymes; for mineral ion binding (amelogenin and enamelin), for modulation of crystal growth (amelogenin, enamelin and ameloblastin), for support of crystal growth (amelogenin and enamelin), for determination of prismatic structure (ameloblastin), for cell signaling (ameloblastin, tuftalin), for control of secretion (breakdown products) and for protection of the mineral phase (amelogenin and enamelin) (Robinson *et al.* 1998).

The crystals first grow in length and then width and thickness. During enamel maturation, complete removal of the inhibitory proteins occurs, which is necessary for the completion (Robinson *et al.* 1989). As the matrix grows in thickness and the environment becomes suitable for crystallization, water and proteins are resorbed. Kallikrein is important in removing proteins from the enamel during the maturation stage (Simmer *et al.* 2009). Without kallikrein, enamel proteins would remain in the matrix, the enamel prism would lack the interlock and fail to grow together, resulting in enamel fracture and a rapid abrading of the function (Simmer *et al.* 2009). Amelogenin forms the bulk of the organic matrix (90%) during the secretion stage and disappears during the process of maturation, while enamelin seems to persist (Termine *et al.* 1980). Enamelin is found in the developing enamel matrix to an extent of 10-15% (Termine *et al.* 1980), however, in mature enamel, the content of enamelin constitutes 50% of the total matrix proteins present (Termine *et al.* 1980).

In the early stages of amelogenesis, the enamel consists of 20-30% protein (Sasaki *et al.* 1997). During the process of mineralization, the proportion of protein is gradually decreasing down to 7% at the beginning of the maturation stage (Sasaki *et al.* 1997). The normal primary enamel is regarded to contain approximately 0.22% protein and the permanent enamel 0.15%, with a similar composition of proteins (Wright *et al.* 1997). The enamel surface of newly erupted teeth consists of water, protein and lipid to approximately 12-14% of the volume (Thylstrup & Fejerskov 1986).

The appearance of defects occurring during amelogenesis is dependent on the stage of the ameloblasts when an injury occurs. Enamel hypoplasia is due to damage to the cells during the secretion stage and

hypomineralization occurs during the late stages of secretion or maturation of amelogenesis (Hu *et al.* 2007; Suga 1989).

1.4 Enamel demineralization

The high degree of enamel mineralization makes the enamel vulnerable to demineralization by acids (Ten Cate 1994). Enamel is to be regarded as dead tissue, with no living cells capable of repairing or reconstructing the tissue after mineralization is completed. However, it is permeable and an ionic exchange may occur between the enamel and outer environment (saliva, oral biofilm) (Ten Cate 1994). The intercrystalline spaces in enamel form an intercrystalline network of potential diffusion pathways, which often are referred to as micropores. The enamel is to be considered a microporous solid (Thylstrup & Fejerskov 1986).

Demineralization is the process of removing the mineral part, permitting access to the organic matrix. This takes place *in vivo* by physiological or pathological pathways (Ehrlich *et al.* 2008). Demineralization and remineralization occurs continuously on the dental surface. This is to be considered as a dynamic process, where the exchange of calcium and phosphate is constantly occurring. The saliva, containing sufficiently high concentrations of calcium and phosphate, makes the enamel more resistant to demineralization (Dawes & Jenkins 1962). Demineralization occurs when the pH is below the critical pH of biofilm (pH=5.1), and remineralization takes place when the pH is higher than the critical pH (Ehrlich *et al.* 2009). Caries is caused by microbially formed acid in the dental biofilm. The first step of tooth caries in the dissolution of the mineral phase in enamel is caused by the generation of a low pH solution. A cavity occurs if the frequency and magnitude of acid production overwhelm the repairing process of remineralization (Ehrlich *et al.* 2008).

A demineralized lesion will appear as a subsurface lesion. This is seen in POLMI, as a located area of higher degree of porosity in the outer part of the enamel, under a porous but intact surface layer. The porosity is highest in the center of the lesion (Thylstrup & Fejerskov

1986). In microradiographs, the subsurface lesion is seen in terms of loss of minerals and as a well-defined lesion, expanding in depth and spreading in a coronal and cervical direction. The surface layer remains intact. In SEM, a distinct area of a different topographic pattern distinguishes the lesion from normal enamel, constituting the demineralized lesion.

Demineralization found *in vitro*, consists of isolation of the mineral phase in biomaterial from the organic matrix (Ehrlich *et al.* 2008). There is an adhesion/decalcification mechanism of acid interaction with human mineralized tissues (Yoshioka *et al.* 2002). The acid will react with the hydroxyapatite in two phases; adhesion and adhesion/decalcification, irrespectively of the crystallinity of the enamel (Yoshioka *et al.* 2002). Further, the rate of diffusion of the organic acid through the intact surface of the enamel seems to be of importance in demineralization (Margolis & Moreno 1992). When minerals are removed by dissolution, the individual crystals diminish, resulting in enlargement of the intercrystalline spaces and increasing tissue porosity (Thylstrup & Fejerskov 1986). Therefore, the enamel becomes more porous. If the total mineral surface formed by the total mass of tightly packed crystals is considered, it is understandable that even a modest loss of mineral from all involved crystals results in a proportionately more pronounced increase in the spaces between the crystals (Thylstrup & Fejerskov 1986). The porosity of enamel is a sensitive indicator for even a slight loss of minerals (Thylstrup & Fejerskov 1986).

1.5 Background

The mineralization of enamel in primary teeth starts *in utero* and continues postnatally. The period of development is limited and so is human tooth material due to ethical reasons, therefore, information regarding the course of events during mineralization is limited. Understanding approximately when, during enamel formation, different elements are incorporated or resorbed, is important for the understanding of normal mineralization and its defects.

The analyses of the neonatal line (NNL) in scanning electron microscopy (SEM), in combination with the X-ray microanalysis (XRMA), have not previously been performed. Neither have comparisons been carried out regarding the diameter of the prenatal and postnatal prisms. The interruption of secretion by ameloblasts at birth always results in a NNL and sometimes in a connecting enamel hypoplasia. Injury to ameloblasts gives rise to certain deviations in the enamel structure. SEM investigations have the potential to clarify the morphological structure in more detail.

There is limited knowledge and information in literature regarding the demineralization of enamel with known chemical content. Therefore, investigations of individual variations of the chemical content and degree of mineralization related to demineralization, may lead to important clinical implications.

2 AIM

The overall aim of this thesis is to add information regarding the structure of primary enamel.

The specific aims were:

- To investigate the neonatal line and compare the prenatal enamel to the postnatal enamel in un-demineralized sections of primary enamel, utilizing polarized light microscopy, microradiography, scanning electron microscopy and X-ray micro analysis of some elements.
- To study the development of the human enamel and especially to investigate the concentration gradients for some elements in primary molars, under different stages of postnatal formation, by means of secondary ion mass spectrometry and X-ray micro analysis.
- To study the morphological and structural properties of enamel hypoplasias in primary teeth.
- To study demineralization in primary enamel in relation to its chemical content and degree of mineralization.

3 MATERIALS AND METHODS

3.1 Material

3.1.1 Tooth bud material *(I, II)*

Mandibular tooth buds from 19 subjects were previously collected for the purpose of a histological study performed in 1996 (Teivens *et al.* 1996). Immediately after extraction, all teeth were put in buffered 4% formaldehyde. The tooth buds were studied for ultrastructural analysis of the neonatal line (NNL). Six central mandibular incisors were chosen from individuals aged 1, 2, 3, 4, 6 and 19 months for analyzing elements during postnatal mineralization (Fig. 3). Identification information was not registered further.

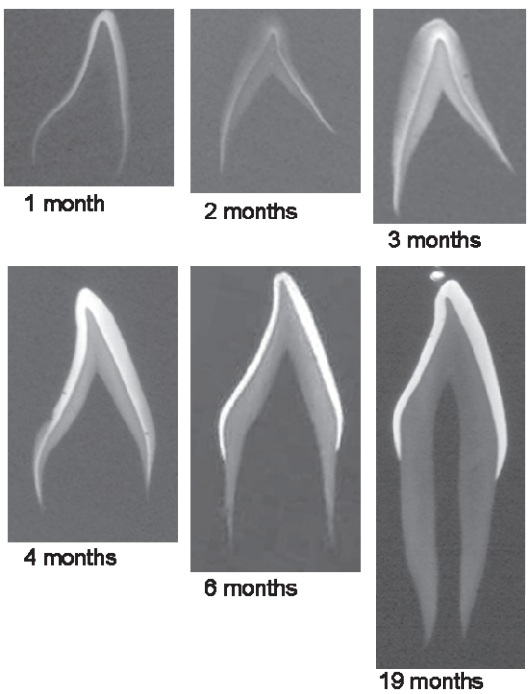

Figure 3. Microradiographs of sections of teeth/tooth buds from different ages; 1 month, 2 months, 3 months, 4 months 6 months and 19 months. Note the growth of the enamel and the root.

3.1.2 Primary tooth material *(I, III)*

Thirty-five exfoliated primary teeth (30 incisors, 5 molars) from healthy, fullterm children were collected. Permission to analyze the teeth was granted from the patients and their parents. The teeth were collected and stored without identification.

Nineteen exfoliated primary teeth (18 upper incisors, 1 molar), with clinically visible enamel hypoplasia, were collected in connection with other studies at the Department of Pediatric Dentistry during the years 2000 to 2008. The teeth were collected and stored without identification in saline with thymol, until preparation.

3.1.3 Patients and teeth (*IV*)

The subjects were comprised of referred patients to the Clinic of Pediatric Dentistry, Public Dental Care, Västra Götaland, Sweden, during the first quarter of the year 2008. The age of the patients varied from 3 to 16.5 years. The reasons for the referrals included extraction of one or more second primary molars. Eighteen children became eligible for the study and 18 primary second molars were collected. Permission and written consent to analyze the teeth were given from the patients and parents.

3.2 Methods

3.2.1 Demineralization of enamel (*IV*)

The teeth were collected for demineralization exposure. Prior to exposure, they were covered with an acid resistant nail varnish (Boots No 7 Colour Lock, Boots, England), leaving a window of 2x2 mm on the buccal surface unprotected.

To create a demineralized lesion, the teeth were covered with an 8% methyl cellulose gel and placed individually in a 30 ml tin, filled with a batch of demineralizing solution (0.1 mol/l lactic acid, pH 5.3) , at a temperature of 37°C for 30 days (ten Cate *et al.* 1996).

After exposure to the demineralizing solution, the teeth were thoroughly rinsed in de-ionized water and photos of the exposed surfaces were taken. The enamel surfaces were visually inspected as qualitative analyses concerning color and structure.

3.2.2 Embedding (*I, II, III*)

The tooth buds were stored in buffered 4% formaldehyde and the remaining teeth were stored in saline with thymol. The teeth and tooth buds were thoroughly rinsed in de-ionized water prior to embedding in an epoxy resin (Epofix®, Electron Microscopy Sciences, Fort Washington, PA, USA). The teeth were stored for at least 24 hours in ethanol.

3.2.3 Sectioning (*I, II, III, IV*)

Prior to sectioning, the samples were placed in a mould and oriented to ascertain a correct cutting direction when mounted in the saw microtome (Fig. 4).

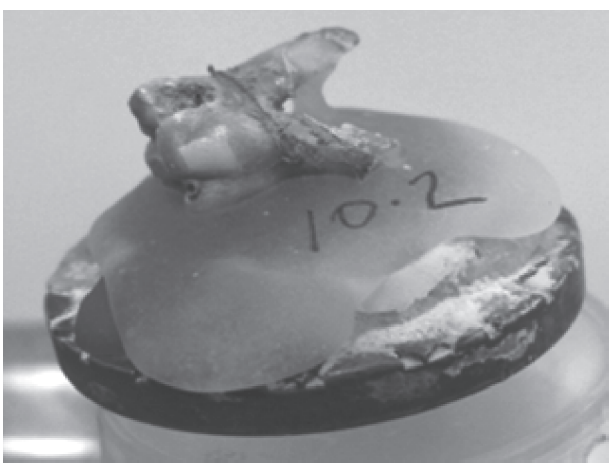

Figure 4. The teeth were mounted in a mould, here unembedded and oriented in accurate direction of sectioning prior to sawing.

Sagittal, un-decalcified sections in a bucco-lingual direction, with a thickness of approximately 100-120 μm, were prepared from the teeth in a Leica SP1600 Saw Microtome (Leica Microsystems GmbH, Wetzlar, Germany) (Norén & Engstrom 1987), always aiming to achieve a central section for further analyses.

The teeth with demineralized lesion were sectioned through the lesion, in bucco-lingual direction.

Sectioning of the teeth with hypoplasia was performed in the middle of the enamel defect. Certain teeth were cut into 2 halves through the enamel hypoplasia in a bucco-lingual direction (Fig. 5).

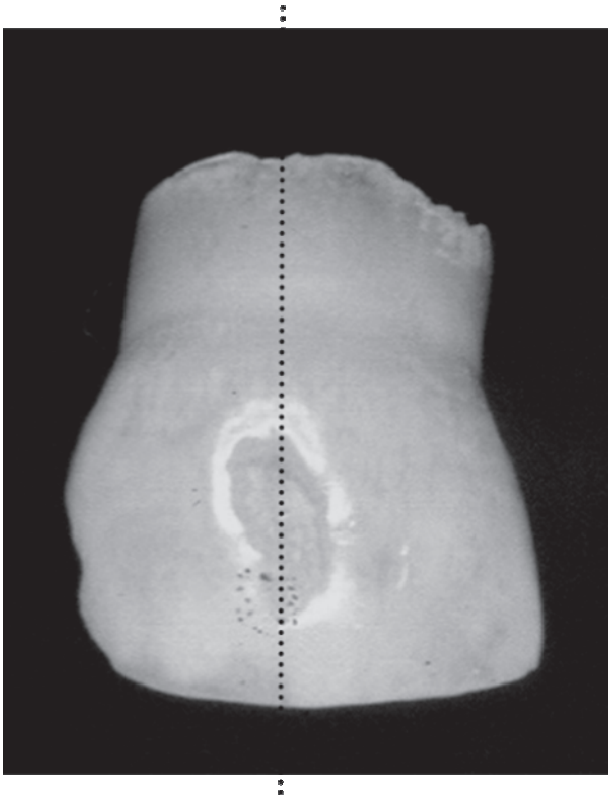

Figure 5. Description of how sectioning of teeth with hypoplasia was performed, in bucco-lingual direction.

In order to keep the sections intact after the first cut of the sample, a drop of Superglue® (cyanoacrylate) (Loctite®, Henkel AG & Co. KGaA, Munich, Germany) and a cover glass were placed on the cut tooth surface. The next section was then cut, preventing enamel breakage of the thin sections. The cover glass was later removed after placing the sections in distilled water for 24 hours.

After sectioning, the samples were placed dry between two object glasses which were secured with tape to keep the sections flat.

3.3 Analyzing methods

The region of interest studied (*Study I, II*) was located on the buccal side of the tooth, with the coronal height identified by the dentin cusp (Fig. 6).

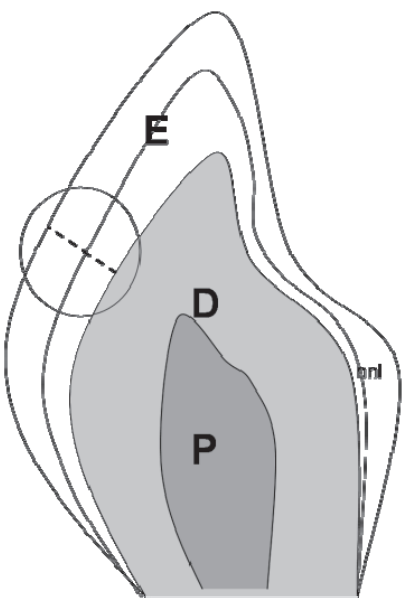

*Figure 6. The region of interest is located at the buccal side of the tooth, the coronal height identified at the dentin cusp. (*E=*Enamel;* D=*Dentin;* P=*Pulp;* nnl=*neonatal line.)*

The region studied in Study IV was on the mid-buccal surface, where the lesion of demineralization was oriented (Fig. 7). The sound enamel located coronal to the lesion was analyzed.

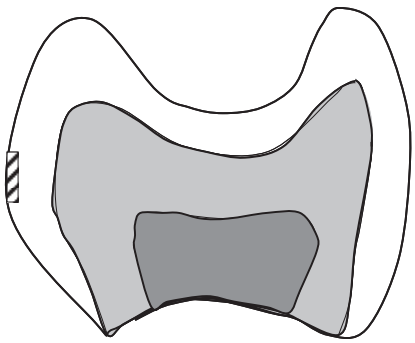

Figure 7. The region studied located on the mid buccal surface, where the lesion of demineralization was oriented. The sound enamel analyzed was located coronal to the lesion.

3.3.1 Polarized light microscopy (*I, III, IV*)

Polarized light microscopy (POLMI) is a contrast enhancing, light microscopic technique which improves image quality. The technique is based on the optical properties of light and by using two polarized filters, the vibration plane of the light waves is determinable.

The microscope is equipped with a turning table and transmitting light. The polarized filters are placed before (analyzer) and after the light passes through the specimen. The polarized filter placed after the specimen (polarizer) is able to rotate and allows the polarized light to pass through the microscope and specimen. If the analyzer and polarizer are placed at a 90 degree angle, all light will be blocked out and the image will appear dark. If a specimen with double refraction is placed between the 90 degree placed filters, an image will appear according to a change of refraction of the transmitting light. The refraction of light depends on the specimen's thickness, orientation of minerals and its birefringence (Fig. 8) (Morad & Ryr 2010).

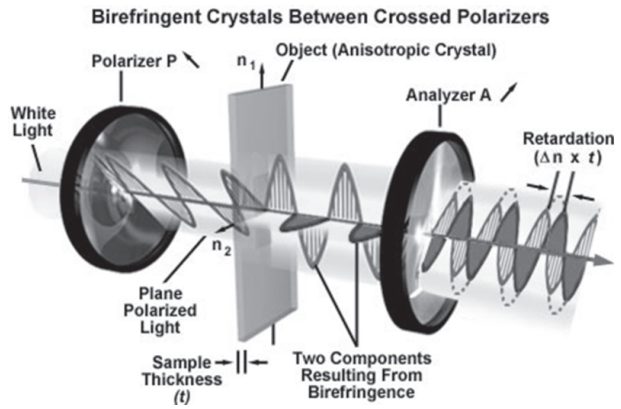

Figure 8. POLMI is based on the principle of the birefringence. The image illustrates a birefringent crystal placed between two polarizers whose vibration directions are perpendicular to each other (and oriented according to the arrows next to the polarizer and analyzer labels). White light entering the polarizer on the left is polarized with an orientation in the direction indicated by the arrow (next to the polarizer label) and is arbitrarily represented by a sinusoidal light wave. Next, the polarized light enters the anisotropic crystal where it is refracted and divided into two separate components, vibrating parallel to the crystallographic axes and perpendicular to each other. The polarized light waves then pass through the analyzer (whose polarization position is indicated by the arrow next to the analyzer label), which passes only those components of the light waves that are parallel to the polarization direction of the analyzer. The retardation of one ray with respect to another is indicated by Δn × t, the difference in speed between the ordinary and extraordinary rays refracted by the anisotropic crystal.
(Image published with permission of Olympus American Inc., Microscopy Resource Center. Originally at http://www.olympusmicro.com/primer/lightandcolor/birefringence.html.)

Enamel is considered to be an anisotropic crystal. Anisotropic crystals interact with light depending on the crystal's orientation of the crystalline lattice (Abramowitz & Davidson 2010). Incoming light is refracted into two light beams in the crystal, each polarized with the vibration directors oriented at right angles and travelling at different speeds. This phenomenon is termed "bi" refraction. The light beams are named the "ordinary beam" and the "extraordinary beam". The ordinary beam travels straight through the crystal and the extraordinary beam proceeds around the ordinary beam. The quantitative calculation of double refraction is called "birefringence" and is defined as the difference of the maximum and minimum of the refraction index of the

sample (Morad & Ryr 2010). When the ordinary beam travels slower than the extraordinary beam, the material is termed negative birefringence (Abramowitz & Davidson 2010).

The appearance of the enamel derives from the transmitted light passing through the full thickness of the section and through the polarized filters. If the polarizer is turned, changes in the appearance of the enamel will depend on the structure of the enamel. Normal enamel has a negative birefringence and will appear blue/turquoise in POLMI, using a λ-filter. In normal enamel, with uniform prism dimensions, the transmitting light is affected by the homogenous structure, which will result in an even appearance and color of the specimen. When the enamel is porous (i.e., hypomineralized) with uneven or heterogeneous prism dimensions, the transmitting light is influenced by the porous enamel's capacity of retardation, resulting in the outcoming light vibrating at a different frequency compared to normal enamel. The porous enamel will then appear in colors from red, yellow to green and opaque, depending on the degree of porosity when using polychromatic transmitting light.

The degree of porosity can be measured by imbibition of the specimen in liquids with different refractive indexes. The refractive index (RI) of hydroxyapatite is 1.62 compared with 1.0 and 1.33 for water and air, respectively. Thereby, the degree of porosity can be calculated. A minor increase in tissue porosity will change the optical properties of enamel so that light will be scattered.

When examining un-decalcified sections dry in air (RI=1.0) in a polarized light microscope, porous areas (pore volume exceeding 1%) appear as a red color. In water (RI=1.33) or ethanol (RI=1.36), a porous area in the enamel with a pore volume of more than 5% will remain red.

All sections were examined dry in air and, after imbibtion in ethanol, in an Olympus polarizing light microscope (Olympus, Tokyo, Japan) using a λ-filter. Images of the sections were taken dry in air and in ethanol with a Leica DFC420 C digital camera using *Leica Application Suite* (Leica Microsystems AG, Heerbrugg, Switzerland).

The depth of the lesions in Study *IV* were analyzed in the *Leica Application Suite* using the change of degree of porosity at the bottom border of the lesion as a marker for the extension of the lesion into the enamel.

3.3.2 Microradiography (*I, IV*)

Contact microradiographs were made using an X-ray tube (type OEG-50 Machlett) with a Cu target and a focal spot of 1 mm, generating a polyenergetic spectrum (Fig. 9). The tube focus was fixed at 242 mm from the recording surface of the specimen. High definition photo plates (HTA photomask, San Jose, CA, USA) were exposed, with the specimen placed directly on the emulsion, to nickel filtered copper radiation, programmed at 20 kV and 20 mA. The plates were developed according to the manufacturer's instructions. The microradiographs were examined in low magnification with a 4x lens in an Olympus light microscope (Olympus, Tokyo, Japan) and further analyzed with *ImageJ*® (Research Services Branch, National Institute of Mental Health, Bethesda, Maryland, USA).

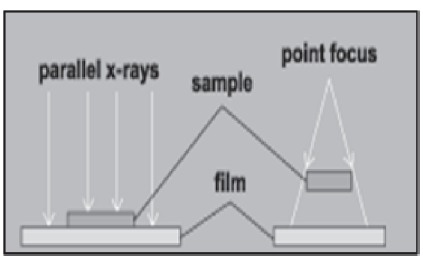

Figure 9. The specimen is placed directly on the emulsion of the film. The distortion of the image is minimal due to parallel incoming X-rays and no distance between specimen and film. The fine resolution is a combination of fine emulsion and exposure of soft X-rays over long duration.

The sections used in Study *I* were exposed at various times depending on their degree of mineralization (tooth buds). In order to achieve relevant information regarding the properties of the enamel, the sections analyzed were of equal and uniform thickness.

Digital images of the microradiographs were taken in an Olympus light microscope and processed in the *Leica Application Suite*. The radiolucency of the sound enamel in each microradiograph was analyzed with *ImageJ*® (Research Services Branch, National Institute of Mental Health, Bethesda, MD, USA), calculating the gray value. By calculating the gray value in the microradiographs along a straight line from the EDJ to the outer surface of the enamel, the degree of radiolucency is measured. Gray value is defined as the brightness of pixels in an image, expressed in integers ranging from 0 (black) to 255 (white), for an 8-bit digital signal. The higher the gray value, the brighter the detail on the image, i.e., the more radio-opaque.

In Study *I*, the gray values at and around the neonatal line (NNL) were calculated with a graph of gray value across the enamel from the surface toward the EDJ. Measurements of the gray value were performed with *ImageJ*®, along two parallel lines through the thickness of the enamel, where a mean value was calculated at each point of the line. Closest to the NNL, at both the prenatal and postnatal side, the gray value was calculated as a mean of the three points closest to the EDJ. The mean values were then compared in order to evaluate the degree of mineralization closest to the NNL.

The sections used in Study *IV* were first analyzed in POLMI, and from the same sections, microradiographs were made and analyzed in *ImageJ*®. The exposure time for the microradiographs of the sections was 75 minutes. Thereafter, the same sections were further analyzed in SEM.

In Study *IV*, lesion depths were measured in the microradiographs, from the enamel surface to the bottom of the lesion (Fig. 10). The bottom of the lesion was observed as a visible transition of radio lucency to radio opacity.

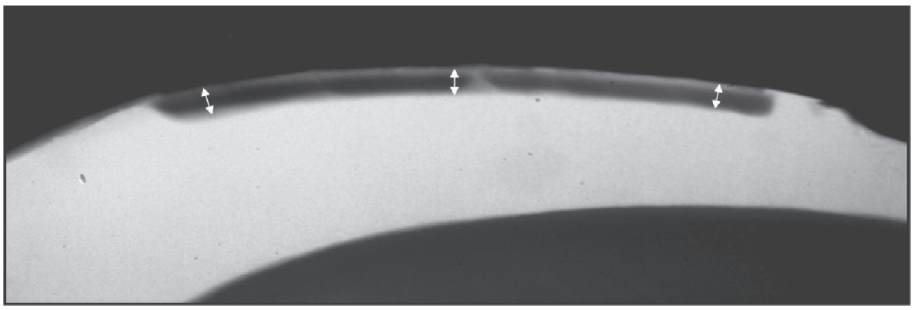

Figure 10. Microradiograph of section with lesion. The depth of lesions was measured at three locations, evenly spread in the lesion, and the mean value was calculated. (Original magnification 4x.)

The gray value was calculated in an area of sound enamel in all specimens in images taken with an Olympus light microscope using the *Leica Application Suite*. The exposure time and settings were reproduced for all sections (possessing similar thickness) in the microradiographs and images by the light microscope. The degree of mineralization and illumination in the microscope was ascertained by measuring the gray scale values over a digital image without any sample. The gray value of the sound enamel and lesion was investigated in *ImageJ*® and the values were compared. The relative decrease of the gray value was calculated as the difference in gray value of the lesion related to the sound enamel in each microradiograph.

3.3.3 Scanning electron microscopy (*I, III, IV*)

To describe SEM in comparison to a light microscope, the main difference is seen in the grade of resolution. A parallel can be made by comparing the image that nuts would create when sprinkled over an opened hand with outstretched fingers, compared with the image that powdered sugar would create over the same hand. The resolution depends on the wavelength of light in the light microscope, while in SEM, it depends on the wavelength of electrons; a 10.000 times shorter wavelength.

The basic principle for a SEM is that a beam of electrons sweeps or scans the surface of the sample, and secondary electrons emitted from

the surface are detected building up an image. The reflected electrons are influenced by the material in the sample, its structure and other factors. The primary electrons create a surface charge which has to be drawn off, or it will mask the possibilities to gain an image. For this purpose, the surface of the specimen is coated with a layer of gold, carbon or any other material with conducting properties.

The electron beam is both a particle with wavelength and also a charged particle (Fig. 11). The beam is directed through the microscope by magnetic fields, similar to optical lenses in a light microscope, via the electromagnets. The electron beam is focused in a very small area. The specimen emits secondary electrons or X-rays due to the radiation of the primary electron beam (Forslind 1981).

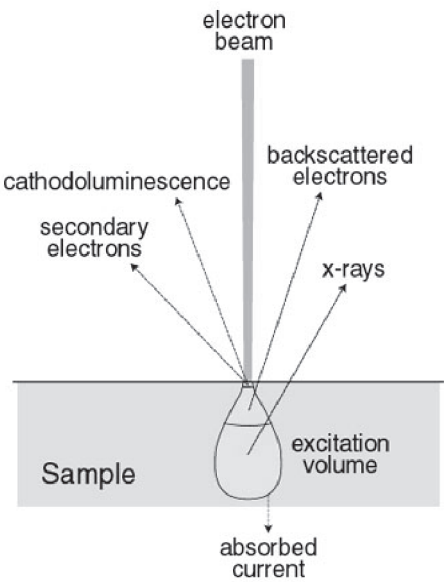

Figure 11. Schematic view of the interaction effects inside the sample when analyzed in SEM. Some the interaction effects due to electron bombardment emerge from the sample. Some, such as sample heating (not shown) stay within the sample. The lines within the interaction volume delineate regions where the effect indicated predominates (see figure). For example, only x-rays emerge from the sample from the deeper parts of the volume. Secondary electrons emerge from the outer surface and backscattered electrons originate from a slightly deeper region.
(Image published with permission from James H. Wittke, PhD, Northern Arizona University, Flagstaff, Arizona, U.S.A. Originally at http://www4.nau.edu/microanalysis/ Microprobe-SEM/Signals.html.)

The image of secondary electrons is given a topographic view of the specimen, as they are reflected from the top atom layers of the specimen and give the best resolution of the surface relief.

SEM can also be used to detect backscattered electrons. Backscattered electrons are the reflected electrons from the primary energy source, reflected by the atoms in a specimen. Backscattered electrons will give information regarding the content of the specimen due to the principle; the larger the nucleus, the more electrons are backscattered. Three dimensional images were created by collecting data from four different detectors. The depth of the structure relief was also measured by this analysis.

The sections examined in SEM were etched for 30 seconds with 30% phosphoric acid and then carefully rinsed with de-ionized water and mounted on sample holders for the electron microscope.

The sections used for the SEM analysis were coated by vapor deposition with gold with a thickness of 15-20 nm. The SEM examinations were carried out in a Philips SEM 515 at 20 kV (Philips, Eindhoven, The Netherlands) and in a field emission scanning electron microscope LEO-1450VP (Gemini IMB, Leo 1530, Oberkochen¸ Germany).

In Study *I*, the diameters of the prisms in the prenatal and postnatal formed enamel were calculated. The calculation was performed as measuring the distance in μm over a set of five prisms (perpendicular to the length axis of the prisms). The mean of a prism was then calculated. The relation of the diameters of prenatally and postnatally formed prims in respective specimen was analyzed.

In Study *IV*, the depths of the lesions were measured in the image of each specimen, from the surface of the enamel to the bottom border of the structural change of the enamel prisms (Fig. 12). The lesion appeared less structured compared with the normal enamel.

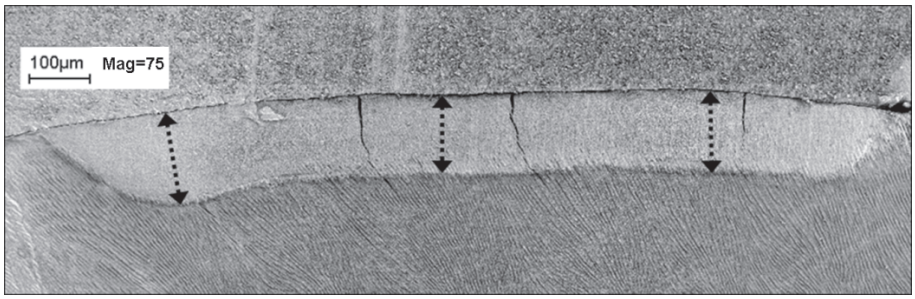

Figure 12. SEM-image of section with lesion. The depth of lesions was measured at three locations and the mean value was calculated.

3.3.4 X-ray microanalysis (*I, IV*)

In SEM in XRMA analysis, an electron beam with an energy between 10-20 kV penetrates into the sample and characteristic X-rays (K-α radiation) are emitted from a pear-shaped volume with a depth of 1-2 µm. Depending on the material analyzed, X-rays may come from as deep as 5-10 µm under the surface, due to higher penetration (less self-absorption) of the X-rays compared with secondary ions (Fig. 11) (Forslind 1981). The X-rays are detected and converted into electronic signals in an X-ray detector and processed by a computer-based software system.

The primary beam excites an electron from the inner shell of an atom in the specimen. Another electron from an outer shell will be attracted to the inner shell. The moving from an outer high-energy shell to an inner low-energy shell creates an X-ray. The X-ray's characterization of each element is explained by each element's unique atomic structure. The X-rays of the elements are identified uniquely from each other.

X-rays give information regarding the chemical content of the specimen and the mass of each analyzed element is presented as weight percent of the total mass, which is 100% (Forslind 1981).

The sections examined in XRMA were prepared by etching for 30 seconds with 30% phosphoric acid. They were then carefully rinsed with de-ionized water and mounted on sample holders for the electron

microscope. The specimens were coated by vapor deposition with carbon with a thickness of 10-15 nm in order to avoid the build-up of a surface charge during the analysis.

The XRMA analysis was carried out in a Philips SEM 515 at 15 kV equipped with an EDAX DX-4 ECON detector (EDAX, Mahwah, NJ, USA) and in a LEO-1450VP, at 12 kV with Quantax 200 (Bruker, AXS, Berlin, Germany) equipped with an XFlash 5030 detector and the *ESPRIT* Software for EDS (Bruker, AXS, Berlin, Germany). The XRMA analysis was performed at a magnification of 250 times, with a working distance of 25 mm.

In Study *I*, the elements analyzed were carbon, nitrogen, sulphur, oxygen, phosphorous and calcium. The measurements were made along two lines through the thickness of enamel, from the surface towards the EDJ. The mean values for each location were calculated. The locations for the XRMA analysis in the enamel of the primary teeth and over the neonatal line are shown in Figure 13.

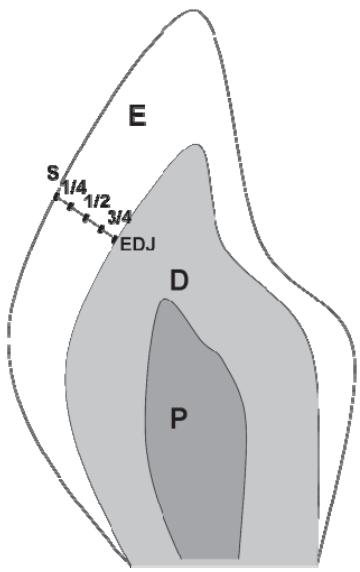

*Figure 13. Locations in enamel where XRMA (line-scans) were analyzed. The first location around 10µm under the surface (*S*), the location closest to the dentin is located 10µm above the enamel dentin junction (*EDJ*). The entire thickness of enamel was measured and the locations of ¼, ½ and ¾ were evenly distributed. (*E*=enamel;* D*=Dentin;* P*=pulp;* NNL*=neonatal line.)*

In order to compare the analyzed elements in demineralized enamel with sound enamel within each section (Study *IV*), two line scans extending over 250 μm, starting at the enamel surface, with 100 measuring points and a count rate of 4 kcps, were made through the most coronal part of the lesion and through the adjacent coronally located sound enamel. The mean and median values of these two measurements were calculated and used for comparison between the lesion and the sound enamel in each section.

Additional XRMA analyses were performed in pre-defined circles (diameter 30 μm), 20 μm below the surface in the lesion and in the neighboring sound enamel. These values reflect the relation of carbon, nitrogen, oxygen, phosphor and calcium in the enamel, and are used for comparison of the relative chemical content in weight percent (wt%) between teeth (Fig. 14). All values are to be regarded as semi-quantitative.

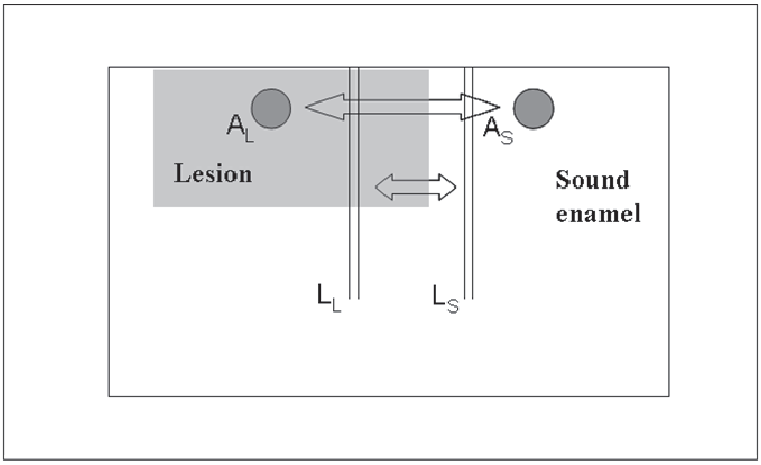

Figure 14. A schematic view of a specimen; the darker area shows the lesion and the white area indicates sound enamel. Two linescans of XRMA (here shown by a set of two parallel lines) were performed through the enamel and through the lesion (L_L) and in the sound enamel (L_S), located coronal to the lesion. The elements measured were C, N, O, P and Ca. A mean value from each point of the lines was calculated. The circles represent the areas in the sound enamel (A_S) and in the lesion (A_L) where XRMA analyses were performed for comparison of wt% of C, N, O, P and Ca between the specimens.

In connection to the XRMA-analysis, the depths of lesions were measured on SEM images and this was compared to the elemental change of calcium in the enamel.

3.3.5 Secondary ion mass spectrometry (*II*)

Secondary Ion Mass Spectrometry (SIMS) is a very sensitive method for surface analyses with detection limits down to ppb levels (Fig. 15). The surface of the sample is bombarded with ions of high energy (primary ions) which leads to the ejection of secondary ions. The secondary ions are extracted into a mass analyzer via a system of magnetic lenses. In the mass spectrometer, which is a combination of an electrostatic analyzer and a magnetic analyzer, the secondary ions are separated by their mass to charge ratio (Fig. 16).

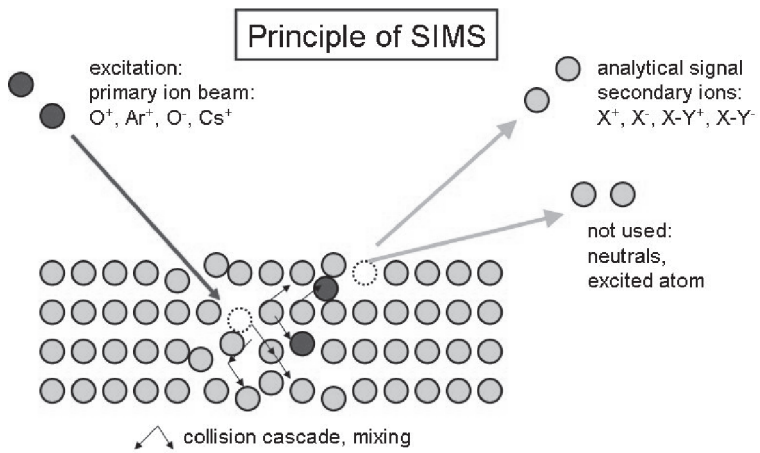

Figure 15. Principle of SIMS. The surface of the specimen is hit by the primary ion source, resulting in ejecting secondary ions from the top atom layers of the specimen.

After mounting of the un-decalcified specimens on sample holders for the SIMS-instrument, the sample surface was coated with gold by vapor deposition in order to avoid the build-up of surface charge from the primary ion beam during analysis.

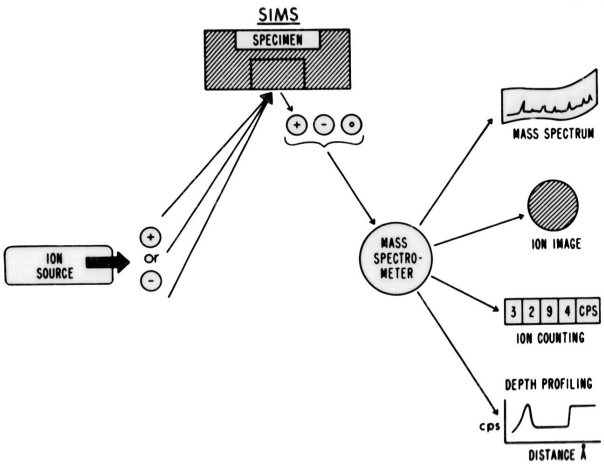

Figure 16. Primary ion source can be either a negative or positive charge, based on which elements are to be detected. The emitting secondary ions are further collected at a detector and categorized by the ratio mass:charge of the elements. SIMS is able to create masspectrometries of the elements, ion images of the selected elements and counting of the emitted secondary ions at their original location in the specimen.

The measurements were performed in a Cameca IMS 3F ion probe (Lodding 1997). The specimen surface was bombarded with O^- to emit secondary ions, which were separated in the instrument according to their mass/charge ratio. The diameter of the analyzed area was 10 μm. Both positive and negative secondary ions were recorded. The measured data for each element was normalized to the corresponding value for the calcium isotope ^{44}Ca in order to compensate for intensity fluctuations due to mineralization irregularities in the sample.

In the SIMS analysis, carbon, fluoride, sodium, magnesium, potassium, chloride, strontium, as well as ^{44}Ca were measured along a line through the enamel with steps of 5 μm (Fig. 17). The SIMS instrument was equipped with a microscope enabling the operator to identify starting and stopping points for the analyses which were then carried out automatically. In order to make comparisons with the XRMA measurements, data from the SIMS measurements was compiled from the corresponding location as in the XRMA analyses (Fig. 13).

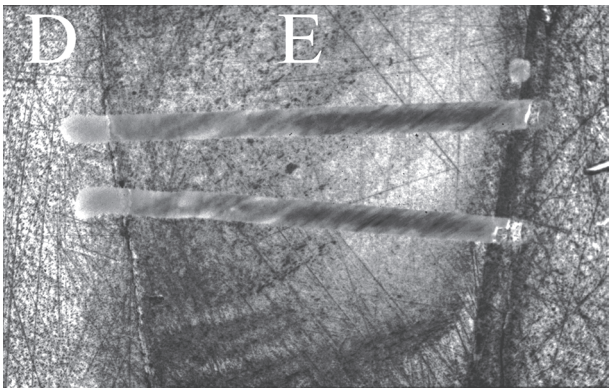

*Figure 17. Traces of SIMS analysis in dentin (*D*) and in enamel (*E*) (Original magnification 4x).*

3.4 Statistical methods *(IV)*

To describe differences in the small sample sizes, attempts were made to study the statistical difference. Data was analyzed using the *Statistical Package of Social Sciences* (SPSS) version 19.0 software program (SPSS Inc., Chicago, IL, USA). The level of statistical significance was set to $p<0.05$.

One-way ANOVA was used to compare the elemental composition between lesion and sound enamel concerning carbon, nitrogen, oxygen, phosphorous and calcium. ANOVA, a non-parametric test, was chosen since a normal distribution of the measured elements was uncertain.

Independent t-test was used to explore differences between the groups of visual appearance and depth of lesion.

Spearman's rank correlation was utilized to analyze the association between the gray value and depth of lesion.

3.5 Inductive analysis *(IV)*

An inductive analysis was performed to find out any relationship between the histomorphological and chemical variables. All data was based from an Excel spread sheet where the values for the different variables were set in columns, each row representing one patient. The variables were age, semi-quantitative wt% of respective element and depth of lesions. The data was imported to the inductive analysis program *XpertRule Miner*® (Attar Software, Lancashire, UK), where the columns represent *attributes* with different *values* (numeric or discrete).

Before the analysis is performed, one of the discrete attributes is chosen as *outcome*. The results are presented in a *hierarchic diagram* (knowledge tree) in which the importance of every attribute in the inductive analysis is specified by its position in the knowledge tree. The higher an attribute is located in the tree, the more important the attribute is for the outcome, and thus the tree shows how different attributes affect the outcome. In the induction process, a knowledge tree is generated by repeatedly splitting the given data set according to different attributes until *terminal points* (leaves) are reached.

The lesion depths (LD) measured in SEM/XRMA (μm) was grouped into three groups: $0<LD<60$; $60\leq LD<100$; and $LD\geq 100$. The three groups represented discrete values and were then chosen as outcome in the inductive analysis. The numerical and discrete data in the Excel file were used as attributes.

3.6 Ethical aspects

Ethical consent using the tooth material used in Study *I, II* and *III* was given by The Ethical Committee at the Sahlgrenska Academy at the University of Gothenburg, Göteborg, Sweden, and registered 343-07.

Study *IV* was approved by The Ethical Committee at the Sahlgrenska Academy at the University of Gothenburg, Göteborg, Sweden, registered 432-08. The participating children and adolescents were

individuals with limited autonomy and dependent on their parents. The patients and their parents received oral and written information regarding the study (one information letter for the participant and one for the parent/care-giver). The information included the purpose of the study, information regarding how participation in the study was voluntary and that all data was to be treated confidentially. No cost or benefits were accompanied with the study. The diagnoses of the teeth were clear and treatment of choice was not influenced due to the purpose of the study. Written, informed consent was obtained from participants and their parents/care-givers.

All study protocols have been followed and were ethically conducted according to the ethical constitution for research, with the general ethical principles described in the Helsinki Declaration (18th WMA General Assembly 2008).

4 RESULTS

4.1 Morphological aspects of the neonatal line *(I)*

The neonatal line (NNL) was found in all of the specimens when examined dry in air in POLMI (Fig. 18). The NNL appeared as a distinct, positively birefringent band extending from the enamel-dentin junction (EDJ) in the most cervical part, toward the enamel surface or around the incisal cusp at the coronal part of the tooth. After water imbibition, the NNL remained positively birefringent, thus the pore volume was 5 % or more.

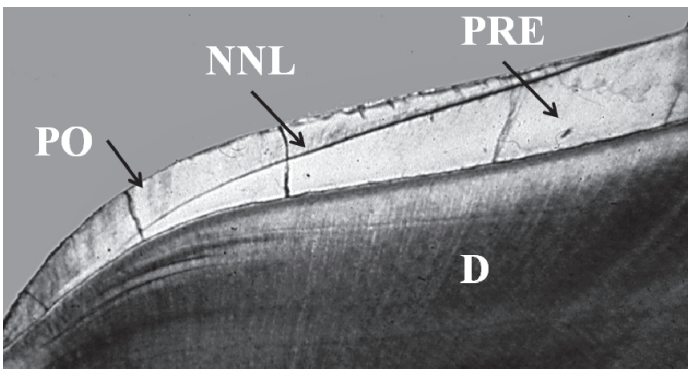

*Figure 18. POLMI image (original magnification 4x) of a neonatal line (*NNL*) in the buccal enamel of an exfoliated incisor. Noticeable is the NNL is starting at the enamel's outer surface and ending at the enamel-dentin-junction in the cervical part of the tooth. (*PO*=postnatal enamel;* PRE*=prenatal enamel;* D*=Dentin.)*

In the microradiographs, the NNL was detectable in 2/3 of the sections (Fig. 19). The NNL appeared in the microradiographs as a thin radiolucent band, confirming its hypomineralized character.

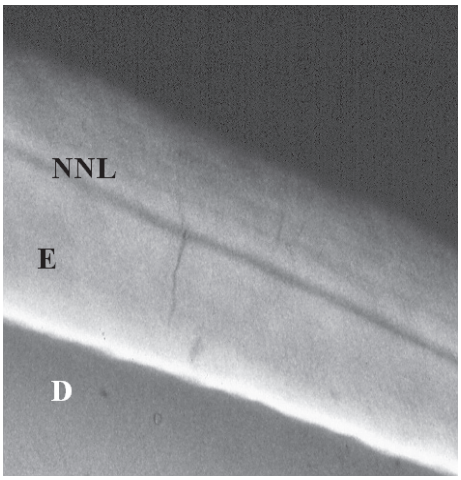

*Figure 19. The neonatal line (*NNL*) in microradiograph (original magnification 40x) of a tooth bud from an individual 3 months of age. The NNL is seen as a radiolucent line in the enamel. (*E=*Enamel;* D=*Dentin.)*

The location of the NNL, seen in the microradiographs, varied in the primary central incisors. In some specimens, it passed around the incisal cusp and ended at the EDJ in the cervical area. In other specimens, the NNL appeared as separate lines on the buccal and lingual sides, respectively, starting at the surface in the coronal part of the tooth and continuing towards the EDJ in the cervical part of the tooth.

In all specimens examined in low magnification (50-200x) in scanning electron microscopy (SEM), the NNL could be seen as a distinct band on the etched surface indicating a change in the prism direction at the NNL, since SEM reflects a topographic image of the surface relief (Fig. 20).

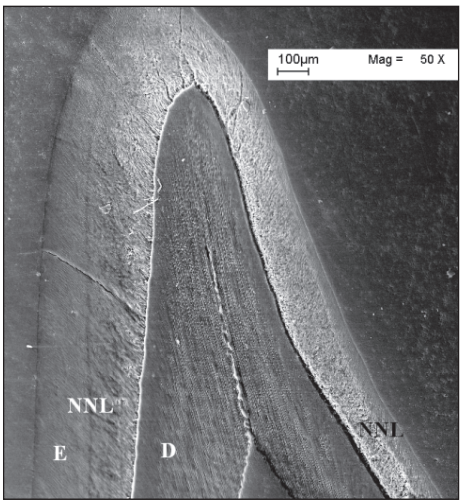

*Figure 20. SEM image over an exfoliated incisor in cross-section. The neonatal line (*NNL*) is seen around the incisal cusp. (*E*=Enamel;* D*=Dentin.)*

4.2 Prenatal and postnatal enamel *(I)*

4.2.1 Measurements of diameter

The diameter of a prism was calculated as the mean value of the distance over a set of five prisms (perpendicular to the length axis of the prisms). The postnatal prisms had, in general, a smaller diameter. The mean prism diameter in the postnatal enamel was 4.80 µm and in the prenatal enamel 5.35 µm, respectively.

4.2.2 Degree of mineralization

The higher the values were for the gray value in the *ImageJ*® graphs, the brighter was the image. The enamel at the surface had a lower gray value compared with the enamel at the EDJ, due to a higher degree of mineralization.

The NNL had a lower gray value and appeared darker (more radiolucent) in the microradiographs compared with the surrounding enamel, as an effect of lower mineral content.

The chemical content of the enamel was analyzed with XRMA across the enamel and the NNL. Intra-individual comparison of each element was made with no noticeable changes in the content of calcium and phosphorous across the NNL. Sodium and magnesium showed a drop in wt% at the location of the NNL in some of the specimens.

4.3 Postnatal mineralization of enamel *(II)*

4.3.1 SIMS analysis

For the interpretation of measured values in the enamel of the tooth buds, it must be emphasized that the thickness of the enamel varied depending on how far the mineralization (age of the child) had proceeded. Thus, the x-axis represents the value of location of measurements performed throughout the entire thickness of developed enamel in each specimen, starting at the EDJ. All values are to be regarded as semi-quantitative and may thus be used for intra and inter-individual comparisons. The enamel of the 19 month old individual was regarded as mature primary enamel.

The content of carbon, fluoride, magnesium, and potassium increased in the outer enamel of the oldest individual, whereas these elements decreased in the younger specimens.

The content of carbon was lower in the enamel of the 19 month old individual, with considerably lower values in the bulk of the enamel, compared with specimens from the younger individuals. The younger individuals had the same level of carbon throughout the enamel. In the outer enamel of the 19 month old individual, the carbon graph showed a peak, which was in contrast to the younger specimens where the outer enamel had a decrease of carbon.

Concerning fluoride, the content in the bulk of the enamel was found to be higher in younger individuals. As for carbon, the highest values

were found at the enamel surface in the specimen from the 19 months individual, in contrast to what was found in specimens from younger individuals (Fig. 21).

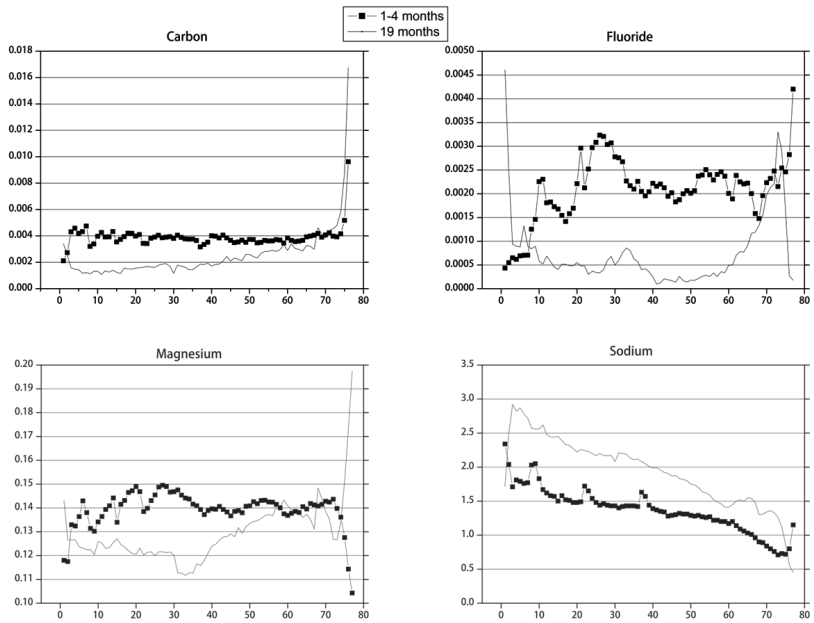

Figure 21. Graphs over concentration of Carbon, Fluoride, Magnesium and Sodium in immature enamel (individuals 1-4 months of age) and in mature enamel (individual 19 months of age). Values on the y-axis represent the logarithmic value of wt%. Values on the x-axis are the distance from the outer enamel surface towards the enamel-dentin-junction.

Magnesium appeared to not alter during the enamel maturation. No age relevant relationship, but a more individual based variation, was seen concerning the magnesium content in the younger specimens. (Fig. 21).

The values for sodium and potassium appeared higher in the 19 month old specimen compared with what was found in specimens from younger individuals. In the outer enamel of the 19 month old individual, the content of sodium had lower values, in contrast to the younger individuals, where sodium had higher values in the outer

enamel. The older specimen showed increased concentrations of potassium also at the enamel surface in comparison to the younger specimens (Fig. 21, 22).

The concentration of chloride was higher throughout the entire thickness of the enamel in the 19 month old, in comparison to younger individuals (Fig. 22).

The content of strontium at the outer surface was at higher levels in the older individual, compared to what was found in specimens from younger individuals. There was no concentration pattern found in relation to chronological ages among the younger specimens (Fig. 22).

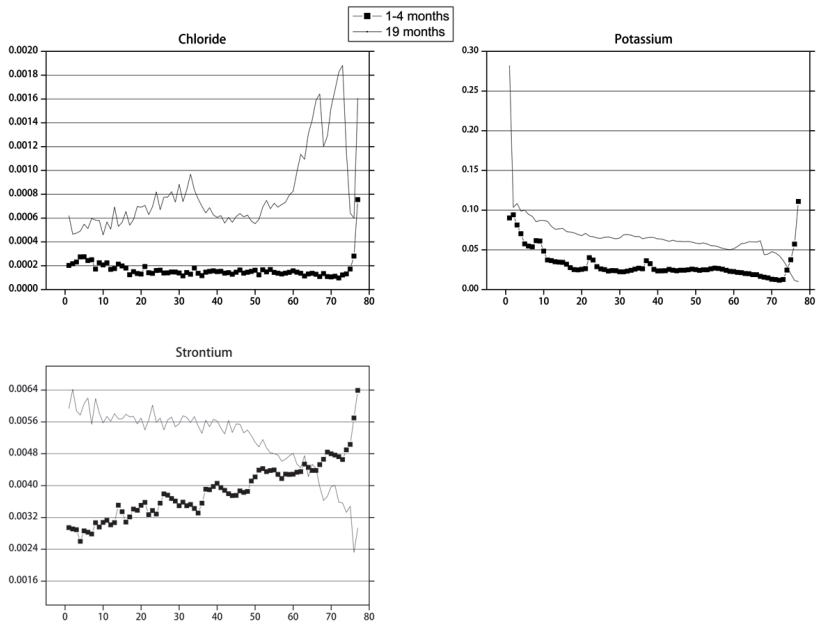

Figure 22. Graphs over concentration of Chloride, Potassium and Strontium in immature enamel (individuals 1-4 months of age) and in mature enamel (individual 19 months of age). Values on the y-axis represent the logarithmic value of wt%. Values on the x-axis are the distance from the outer enamel surface towards the enamel-dentin-junction.

The concentration of the measured elements differed between the analyzed specimens. In order to visualize how postnatal mineralization progresses, graphs were constructed from the collected data. Further, the mean values for the element concentrations in enamel from the individuals from 1-4 months old were compared with the enamel of the 19 month old specimen.

4.3.2 Growth of enamel

The enamel thickness increased from 205 µm at 1 month of age to 385 µm at 19 months of age (Fig. 23). Full thickness of the enamel was reached between 3 and 4 months of age.

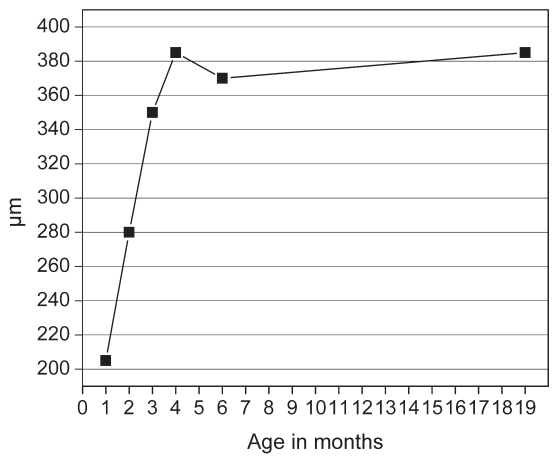

Figure 23. Graph of buccal enamel thickness of mandibular central incisors during enamel development, related to age of individual. The location of measurement was located in line with the most coronal part of dentin.

4.4 Enamel hypoplasia *(III)*

The clinically visible surface defect of the enamel's volume, enamel hypoplasia, is due to a local quantitative defect in the enamel formation. The hypoplasia possesses rounded borders and the base, constituting the floor of the defect, has a rough surface.

A congruence was seen between the findings in POLMI and SEM regarding the morphological structure of the enamel hypoplasia. The border of the hypoplasia, i.e., the neighboring cervical enamel, appeared rounded and smooth (Fig. 24). There was no difference in appearance of the borders of an enamel hypoplasia located in incisors or molars.

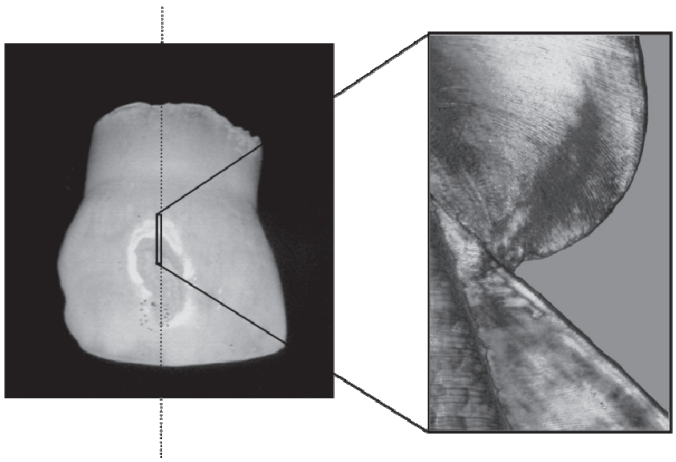

Figure 24. Image of a hypoplasia at the buccal surface of a primary incisor. The enlargement is a POLMI image of the cervical border of the hypoplasia (original magnification 10x). The reduced amount of enamel is seen, following an incremental line. The cervical enamel, fully developed in volume, has curved prisms establishing the rounded borders of the hypoplasia defect. The degree of porosity in the enamel with curved prisms is reduced in comparison to enamel with normal prisms.

The cervical border of the enamel hypoplasias was found in connection to incremental lines. Macroscopically, the more shallow hypoplasias were seen as bands cross the crown in mesial-distal direction and surrounded with enamel of normal appearance.

In POLMI, the cervical rounded border region at the entrance of an incremental line had a yellow-reddish color dried in air. This changed to a turquoise color after water imbibition, indicating a pore volume distribution of <5%.

The enamel at the bottom of the enamel hypoplasia was reduced in volume and was more rough and porous compared with a normal enamel surface (Fig. 25). No sign of an aprismatic enamel layer was found.

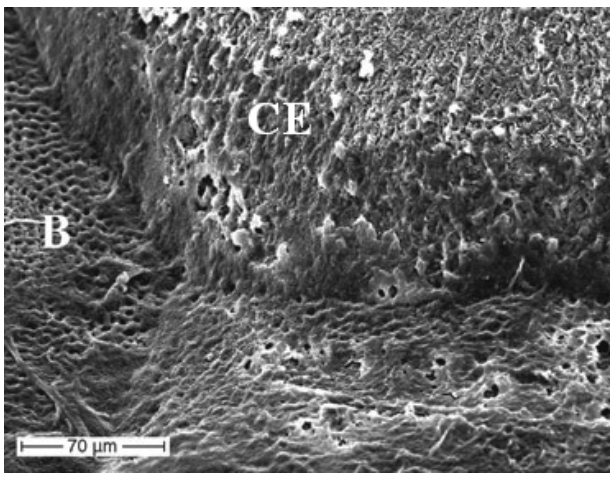

*Figure 25. SEM image of hypoplasia. The base (*B*) of the hypoplasia is seen to have reduced a volume of enamel and is more porous than the rounded cervical enamel (*CE*). The more porous enamel, without an aprismatic surface layer, is usually found at the outer surface of normal enamel. (Magnification 400x.)*

In POLMI, the formation of reparative dentin was found corresponding to the area of more porous enamel at the bottom of the hypoplasia. This indicates a possible pathway for toxins or bacteria from the oral environment through the volume-reduced and more porous enamel, into the dentinal tubules.

In the cervical part of the hypoplasia, at the intersection with the neonatal line, the enamel prisms showed a distinct rupture. The prenatal prisms had concave endings while the postnatally formed prisms had convex endings (Fig. 26).

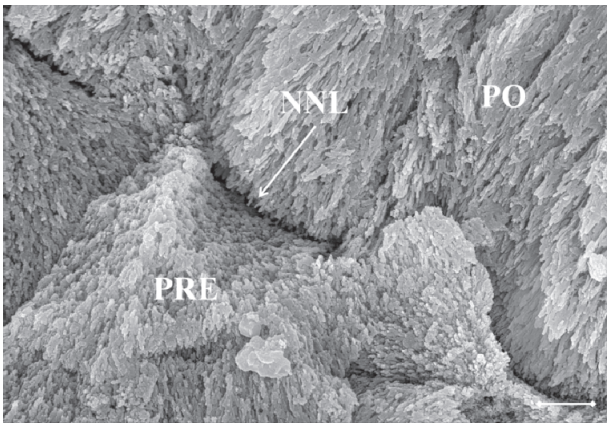

*Figure 26. SEM image of un-decalcified sections of a primary incisor showing concave prenatal and convex postnatal prism endings (Magnification 10 000·; bar=1 µm). (*NNL= *neonatal line;* PRE=*prenatal enamel;* PO=*postnatal enamel.)*

4.5 Artificial demineralization of primary enamel *(IV)*

4.5.1 Morphological appearance and lesion depths

The appearance of the enamel surface where the lesion was located differed between the teeth. Therefore, the teeth were grouped into two groups according to the appearance of the enamel surface; chalky and rough (n=10) and chalky/tooth colored and glossy (n=8). The grouping was based only on the macroscopical appearance (Fig. 27).

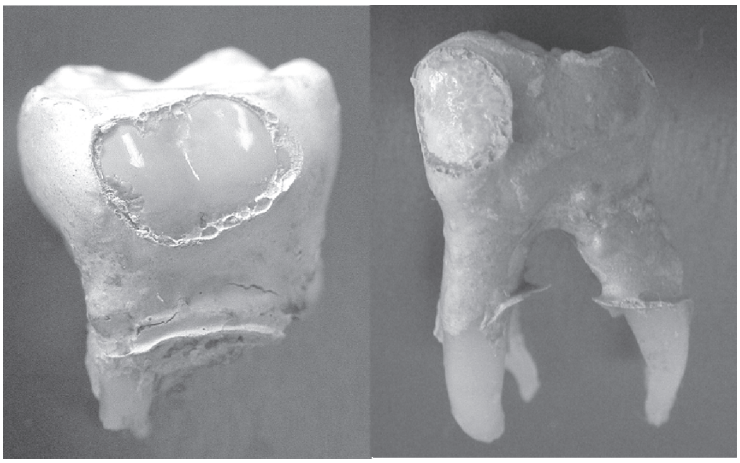

Figure 27. Teeth after demineralization. The surface appearance of the demineralized window was categorized as either chalky/tooth colored and glossy or as chalky and rough.

Within the enamel, the spread of the lesion is observed to be defined by prism boundaries, in a coronal and apical direction. The depth of the lesion is seen to be consistent even throughout the extent of the lesion. This is clearly seen in the microradiographs and SEM images. Depths of lesions were measured in POLMI, microradiographs, SEM and SEM/XRMA (Table 1).

The lesion depths were analyzed in relation to their microscopical appearances (Fig. 28). A correlation in teeth with chalky and rough appearance and having deeper lesions, whereas the teeth having a glossy enamel surface had shallower lesions. The degree of mineralization of the enamel surface has an obvious importance for aspects of demineralization. The more porous a surface, the deeper the lesion which consequently will result in an even more porous surface and thereby, a faster demineralization.

*Table 1. Mean of depth of lesions (in micrometer) in all specimens, measured in polarized light microscope (*POLMI*), microradiographs (*MRG*),* SEM *and* XRMA *images.* Age *in years of the individuals at the time of tooth extraction. Appearance of lesions;* 0*=chalky and rough surface,* 1*=chalky and smooth surface,* 2*=normal color with a smooth surface.*

	Methods (depth in micrometer, age in years, appearance see legend)					
	POLMI	**MRG**	**SEM**	**XRMA**	**Age**	**Appearance**
1	74	71		57	13	0
2	110	46	58	48	13	2
3	87	82		83	5	0
4	112	49	47	70	5	1
5	91	40		89	5	0
6	66	44	78	71	8	0
7	57	54	70	75	6	0
8	94	53	51	73	5	2
9	99	99	130	112	7	0
10	56	43		70	7	1
11	38	25	31	40	13	2
12	74	72		110	17	0
13	87	37		66	6	1
15	68	59		85	6	1
16	77	38	46	63	3	0
17	81	73		115	6	0
18	109	75		52	15	1

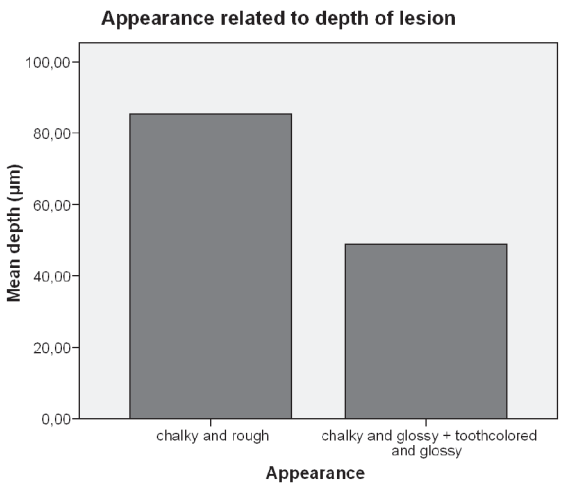

	appearance	N	Mean	Std. Deviation	Std. Error Mean
Depth in EDX (µm)	chalky and rough	9	86,11	21,871	7,290
	chalky and glossy + toothcolored and glossy	8	63,00	14,957	5,288

Figure 28. Appearance of surface related to lesion depth. The group with more affected (chalky and rough) surface showed deeper lesion depth.

4.5.2 Polarized light microscopy

The loss of minerals affects the orientation of crystals and influences the appearance in POLMI. In the more porous lesions, light will diffract differently. The extension of the lesion, in coronal and apical directions, is clearly defined by the prism boundaries. The depth of the lesion was consistent in all parts of the specimen.

In sound enamel, the enamel surface and the enamel zone below the lesion appeared negatively birefringent when examined dry in air. The lesion depth varied between the specimens. Deeper lesions were seen as a fairly uniform demineralized zone, with a positive birefringence deep to a negatively birefringent surface layer. Shallower lesions were seen as a dark band just under the surface layer (Fig. 29).

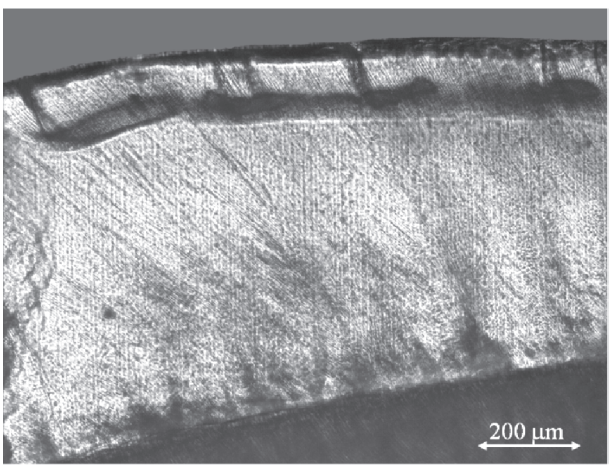

Figure 29. POLMI image, at 4x. The lesion is seen as a uniform demineralized zone, with a positive birefringent bulk below a negatively birefringent surface layer. At the lesion front, a zone with a higher degree of demineralization is seen.

4.5.3 Microradiography

In the microradiographs, the increased pore volume of the lesion is observed as a loss of mineral below the relatively unaffected surface zone. In principle, the loss of mineral is most pronounced in the body of the lesion, with a gradual decrease of minerals from the above intact surface layer. A lesion was detectable in all microradiographs. The

lesion had a fairly consistent depth within each specimen, however, the depth varied between the specimens.

The gray value throughout the lesion and into sound enamel, underneath the lesion, was distinct and easy to interpret. When comparing the gray value along two lines, one throughout the enamel with a lesion and the other throughout sound enamel located coronal to the lesion, the gray value decreased in the lesion (Fig. 30).

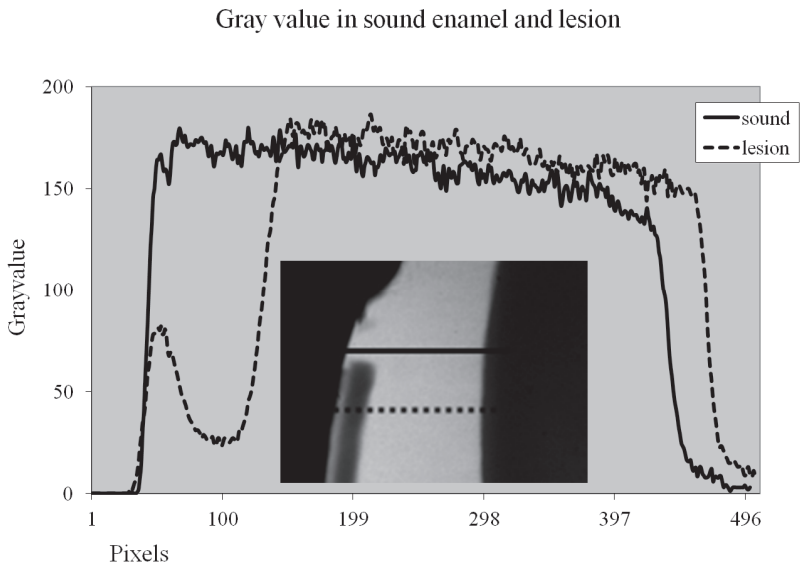

Figure 30. Image from a microradiograph and graph of gray value related to the image. Dotted line through the lesion and full line through the sound enamel.

The gray value of the sound enamel and the lesion measured in the microradiographs differed between the specimens. Variations in the gray values, found between sound enamel from different individuals, were interpreted as individual variations in the degree of mineralization.

The specimens with a deeper lesion showed a lower relative gray value. The sound enamel in the group of specimens, having deeper

lesions, had a lower gray value compared to sound enamel in specimens with more shallow lesions. The gray values of the lesions were similar regardless of the depth.

4.5.4 Lesion depth SEM/XRMA

The lesion was seen as a homogenous change of structure with well-defined borders. The lesion appeared with less structure compared with sound enamel (Fig. 31). However, the prisms were still discernible, but no crystals were detectable in the lesion. The lesion depths measured in SEM and XRMA are shown in Table 1.

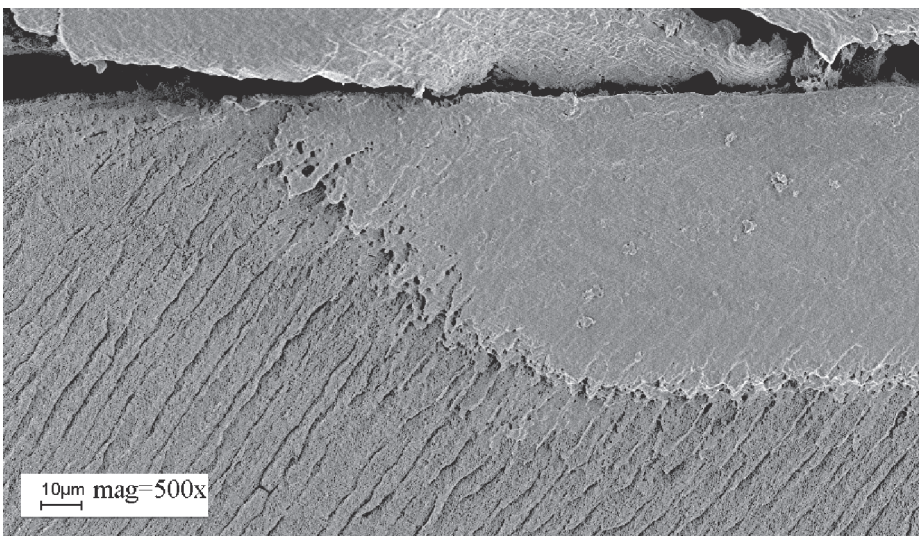

Figure 31. SEM-image (magnification x500) over well-defined expansion of a demineralized lesion. The topographic appearance of the lesion differs from sound enamel.

All of the shallow lesions (0-60 µm) were found among individuals older than 8 years, however, no statistical significant correlation was found.

4.5.5 X-ray micro analysis

In order to investigate differences in the chemical content between mesial, buccal and distal, or mesial and distal sides of primary tooth enamel within the same tooth, nine teeth from nine individuals were used for the XRMA analyses. Sections were cut in a sagittal or radial direction to a thickness of 100 μm and coated with carbon by vapor deposition. The XRMA analyses was carried out in the same way as in the main study, measuring the content of C, N, O, P and Ca in the enamel at 5 locations over a line from the enamel surface toward the enamel-dentin junction. No differences were seen in the chemical content of C, N, O, P or Ca within the individual sections between the different locations of the surfaces of the tooth. Inter-individual differences in chemical content of N, O, P and Ca were observed ($p<0.05$) in the location closest to the enamel surface. However, variations between the different individuals were larger compared with what was found within the enamel of an individual.

Table 2. Mean wt% of carbon, nitrogen, oxygen, phosphorous and calcium in sound enamel and lesions.

Chemical content in normal enamel and in lesions (weight%)										
	Carbon		Nitrogen		Oxygen		Phosphorous		Calcium	
	Sound	Lesion	Sound	Lesion	Sound	Lesion	Sound	Lesion	Sound	Lesion
Mean	6.21	23.33	2.04	5.49	41.02	40.72	15.90	11.34	34.82	19.13
Median	5.68	18.74	1.74	5.45	39.58	40.90	15.54	11.16	30.06	18.84
STD	2.13	11.95	1.02	1.67	3.68	6.30	1.30	1.30	4.18	7.97

The chemical content of sound enamel varied between different individuals. The variations of elements were even more pronounced in the lesions (Fig. 32). The mean ratio of Ca:P was 2.1 in sound enamel and 1.7 in the lesion. The mean values and the corresponding standard variations of the semi-quantitative wt% of measured elements, from all specimens, are illustrated in Table 2.

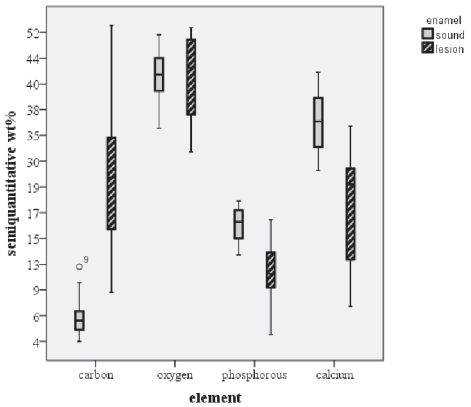

Figure 32. Box-plot over distribution of semi-quantitative elemental composition in sound enamel and in lesion.

As for the other measured elements, the concentration of carbon in sound enamel differed between the individuals. The higher the content of carbon, the deeper was the lesion. In the deepest lesions, the carbon content had a value higher than 7wt%. The graph in Figure 33 illustrates the individual specimens' data of chemical content and lesion depth.

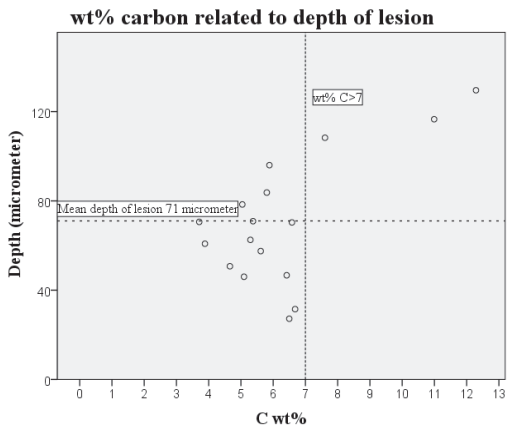

Figure 33. Plot of the wt% of carbon in sound enamel related to depth of lesion. The specimens with a wt% of carbon >7% have deeper lesions.

In the enamel underneath the lesion, at the border of the lesion facing normal enamel, the lower level of calcium rapidly increased to a normal level. A prominent change of the content of carbon was also

seen at the border. The lesion had a higher content of carbon compared with normal enamel. The lesion depths according to normalized content of calcium and carbon were in agreement with the depth of the lesion visible on the SEM/XRMA image (Fig. 34).

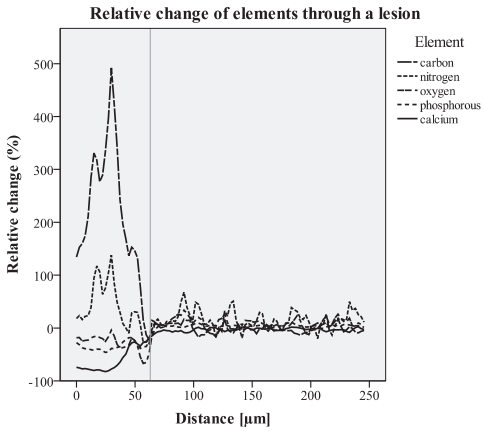

Figure 34. Relative change of measured elements through enamel with a lesion from one tooth. The vertical line indicates the lesion depth according to SEM/XRMA (61 µm) of this specimen.

4.5.6 Inductive analysis

The inductive analysis revealed that the attribute "Age" (age of the patient at the date of extraction) was the most important attribute for the outcome of "lesion depth" measured in SEM/XRMA (Fig. 35). The inductive analysis revealed that the break point was at 8.2 years of age. Thus, all other attributes were redundant. The older the patient, the more shallow the lesion. The lesion depth was between 60 and 100 µm for 83% of the patients younger than 8.2 years of age, while 80% of the lesions were between 0 and 60 µm among the patients older than 8.2 years of age.

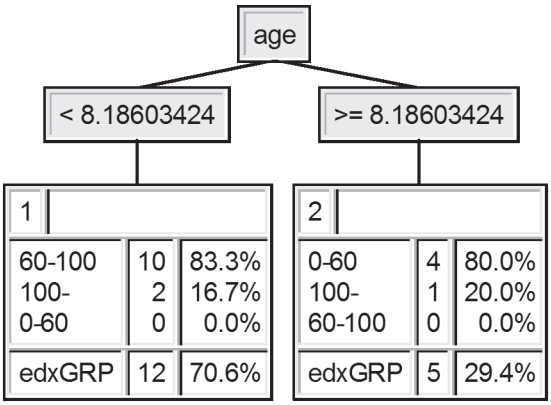

Figure 35. Knowledge tree generated in XpertRule Miner. At the top of the tree is the attribute "Age" located with the break points for the two end leaves with the group names, frequency within each group and percentage of correctly classified examples. The last row shows the total frequency of examples and the overall correctly classified examples.

5 DISCUSSION

This thesis has focused on the description of some morphological findings in primary enamel and chemical changes during primary enamel formation. The main findings were that the neonatal line is a hypomineralized structure, sometimes with a rupture in the continuing prisms. The prenatally and postnatally formed prisms differed in diameter within the same individual. Enamel hypoplasia is a quantitative defect in the enamel, displaying a rough surface at the bottom of the hypoplasia. The rounded borders of the defect are an effect of bending of the full length prisms. The bended prisms were of normal morphology, however, with increased interprismatic areas, seen as more porous enamel in POLMI. No differences in the morphological appearance in hypoplasias of incisors and molars were seen.

The chemical composition in primary enamel differs to some extent between individuals. The degree of mineralization and the chemical content of enamel influences the demineralization of enamel. Demineralized lesions were deeper in the more porous sound enamel and enamel containing more carbon. Individuals older than 8.2 years had shallower lesions, interpreted as a posteruptive effect (oral environment) of the mineralization of the enamel surface.

5.1 Tooth material

The number of analyzed teeth was limited, however, the tooth bud material is unique, since it is almost impossible today to collect tooth material from deceased children, due to ethical reasons. Therefore, it is of importance to gain as much information as possible using different analytical methods.

Primary tooth material for morphological analyses of enamel hypoplasia represents an enamel aberration with a low prevalence of hypoplasias. The teeth have been collected in connection with other studies during a number of years.

For the study of demineralization of primary enamel, the collected primary molars were limited in number.

5.2 Methodological considerations

There is no evidence or reason to believe that the storage media used (ethanol, buffered formaldehyde, saline and saline with thymol) has had any influence on the morphological structures or in the main chemical components of the enamel. Irrespective of the storage media, all teeth have been exposed to 70% ethanol for at least 24 hours prior to embedding in epoxy.

In order to correctly interpret the findings in POLMI and in the microradiographs, the sectioning of the teeth aimed to achieve plano-parallel sections with the same thickness.

5.3 Polarized light microscopy and microradiography *(I, III, IV)*

Examinations in polarized light microscopy followed a protocol based on methods previously described in the literature (Gustafson 1959). The examination of each specimen was performed at least twice at two different locations.

The negatively birefringent enamel seen in POLMI contains more minerals than positively birefringent enamel (Allan 1959; Gustafson 1959). The degree of porosity can be investigated by imbibition of the specimen in various solutions with different refractive indexes (RI). In the present studies, the enamel was examined dry in air (RI=1.0) and in ethanol (RI=1.36), which shows information regarding the porous areas in the enamel, and whether they have a degree of porosity of more than 5%.

The microradiographs were exposed to the same kV and an Al-stair was used on each microradiograph as a reference. The development

and fixation of the exposed films were carried out according to the manufacturer's instruction in order to minimize possible artifacts.

5.4 Scanning electron microscopy and XRMA *(I, III, IV)*

SEM is a surface analytical technique widely used for morphological studies of dental hard tissues. X-ray micro analysis has the advantage that measurements can be carried out with a full location control within a specimen. The sensitivity and detection limits for measurements in dental hard tissues restricts its use to a few elements but constitutes a reasonably accurate method for the analysis of, e.g., Ca and P. The measured values, given as a weight %, are regarded as semi-quantitative since an appropriate standard for enamel and dentin is lacking. Nevertheless, the values may be used for comparisons within a specimen and also between specimens. A calculation of the ratio Ca:P gives an indication of the validity of the measurements.

5.5 Secondary ion mass spectrometry analysis *(II)*

The SIMS-technique has long been used for elemental analysis in dental hard tissues and is a sensitive method, especially for light elements. One major advantage is that measurements can be performed with high accuracy in morphologically predefined areas and that the values for the measured elements can be compared within a specimen as well as between different specimens. However, the SIMS-techniques are time-consuming and expensive which limits its use to some extent.

5.6 Ethical considerations

5.6.1 Tooth buds (*I, II*)

The tooth buds were part of a previous medical-forensic study and collected for a histo-morphological study. The data connected to the tooth buds was medical without any possibilities to relate any sample to a specific patient. As the regulations and rules for histological studies of teeth changed since the first study, a new ethical application was performed. The Ethical Committee at the Sahlgrenska Academy at the University of Gothenburg, Sweden, registered 343-07, approved the analysis of the unidentified tooth material previously collected.

5.6.2 Primary teeth *(III, IV)*

The primary teeth for the histological analysis of enamel hypoplasias were collected over several years. Teeth were voluntarily given by the child and parent, when teeth were exfoliated. The collected teeth were stored without reference to any patient.

The study of primary incisors for the demineralization studies was subjected to an ethical application and approved by the Ethical Committee at the Sahlgrenska Academy, University of Gothenburg, Sweden, registered 432-08. The patients and their parents were given written information regarding the study. Participation was voluntary and written consent was given. No form of reimbursement was made.

5.7 The neonatal line *(I)*

The neonatal line was found in all specimens when analyzed in POLMI and almost all neonatal lines were detected in the microradiographs. The width of the NNL might influence the detection. The width of the NNL varied between individuals (Norén *et al.* 1978; Ranggard *et al.* 1994). The analysis in POLMI reflects the degree of porosity in the specimen, while microradiographs reflect the

degree of mineralization. The NNL may thus be described as an incremental line of more porous and less mineralized structure.

The chemical data from the analyses across the NNL showed only minor deviations compared with normal enamel. Analyses across an incremental line demands very close points of analyses in order to show variations.

The diameter of prenatally formed enamel prisms was larger compared to the postnatally formed prisms. There are several studies made on primary enamel reporting the prenatal enamel being more uniform and containing less defects compared to postnatal enamel (Gustafson 1959; Massler & Schour 1946).

Hypomineralization, as seen in fluorosis, is a result of an excessive amount of fluoride during the secretion stage (den Besten 1986). The NNL is also a hypomineralized structure worth considering since it is a response due to events during the secretion stage – in congruence with this is the frequent finding of hypoplasia in regions of the NNL.

5.8 Enamel hypoplasia *(III)*

The examination of enamel hypoplasia and its rounded borders with a scanning electron microscope describes the morphological micro-structure. The enamel prisms adjacent to the hypoplasia were of normal length. Due to missing full-length prisms in the hypoplasia, the neighboring full-length prisms are bent, caused by lack of support of the full-length prisms. Thereby, a smooth and rounded curvature will appear from the enamel of normal thickness toward the bottom of the hypoplasia. The bent prisms are fully mineralized, however, due to the curvature of the prisms, the neighboring enamel is less densely packed and appears to be slightly hypomineralized at the border of the hypoplasia.

The rough bottom of an enamel hypoplasia indicates an abrupt interruption in enamel formation and therefore, appears more porous and hypomineralized than normal enamel. No aprismatic layer was

found on the bottom of the enamel hypoplasia as can be found on a normal enamel surface. Normally, the outer surface of enamel has an aprismatic layer (Whittaker 1982). Analysis of the base of hypoplasia is to be regarded as hypomineralized enamel (Fearne *et al.* 1994). Hypoplasia is damage to the ameloblast during the secretion stage where the ameloblasts are detached from the forming enamel surface or degenerated (Suga 1989). The ameloblasts seem to recover and maturation of enamel is taken place, though a more hypomineralized enamel is developed compared to normal enamel (Fearne *et al.* 1994; Suga 1989). The influence on clinical aspects shows that enamel hypoplasia appears to be a risk factor for caries (Hong *et al.* 2009; Oliveira *et al.* 2006).

Hypocalcemia is proposed to be a dose-dependent main factor behind enamel hypoplasia (Nikiforuk & Fraser 1981; Ranggard *et al.* 1994). The close location of the enamel hypoplasia and the NNL raise considerations regarding hypocalcemia of the child at the period of birth, indicating the NNL might be a result of hypocalcemia. Ameloblasts are affected at the secretion stage where hypoplasia is formed. Since the ameloblasts are disrupted in incremental lines, as in the NNL, these ameloblasts are also affected at the secretion stage (Gustafson 1959; Suga 1989). Very few of the ameloblasts respond to stimuli, which in turn, results in hypoplasia. Therefore, is reasonable to believe that the (dose-dependent) injury is of short duration. In the sub-stage of the secretion stage, the ameloblast are presumably more sensitive to damage by a hypocalcemic situation. Additionally, the diameter of the prisms in postnatally formed enamel was smaller than the prenatally formed prisms. This may indicate recovery of the ameloblasts from an injury caused by hypocalcemia at birth.

5.9 Postnatal mineralization of enamel *(II)*

Analyses were made across the enamel in the region of the most coronal part of the dentin. Analyzing enamel at three location on the buccal side of the tooth, in at least three levels, might have given more information regarding the progress of the process of mineralization.

The analyses were made along one line in all specimens since the SIMS method is cost and time-consuming.

The enamel of primary second molars is mineralized by the end of the first year of life (Lunt & Law 1974). Therefore, at nineteen months of age, the primary second mandibular incisor is to be considered fully developed, according to the schematic view of the chronology of developing primary teeth (Massler & Schour 1946).

The compound graph of the analyzed elements is an attempt to make the concentrations of elements in immature and mature enamel more explicit. Therefore, the graph may be interpreted as the progress of maturation in relation to the chemical content in the maturation stage of mineralization. The concentration of elements in enamel from the individuals aged 1-4 months were compared to enamel from the 19 month old individual in the compound graph. The specimens from the 1-4 month old children were considered to constitute one group, based on these specimens possessing immature enamel, still under development. A mean value of each element was calculated from the young individuals. It must be observed that the calculated values represent a range of individual concentration of each element as well as a range of maturation of the secreted enamel matrix. Data from the mature enamel (19 month old specimen) was from one single individual and cannot be used to generalize for the total population. The graph of the younger specimen represents four individuals, the 19 month old is data from one individual.

The maturation stage in the investigated enamel seemed to involve all the elements looked at (Study *II*). The specimens were from different individuals, and the pattern in the graphs of each element should be viewed in consideration of both individuality and the enamel's stage of maturation and mineralization.

The concentrations of potassium seem to be individual, no correlation to chronological ages could be observed in the younger specimens.

The peak of fluoride in the enamel surface of the 19 month of age specimen is to be considered as a result of eruption of the tooth and exposure to the oral environment. The enamel surface is likely to

become affected by the oral environment as soon as the tooth erupts. The oral bio film is supersaturated with calcium, inorganic phosphate and fluoride compared to the enamel (Fejerskov *et al.* 1996; Thylstrup & Fejerskov 1994).

The development of enamel occurs approximately the same period in all patients. Some individuality may occur during the development regarding specific timing and effects from the environment (Lakomaa & Rytomaa 1977; Nikiforuk & Fraser 1981). The differences found in the elemental composition in normal enamel between individuals are a reflection of this. To which degree this individuality affects enamel clinically, remains to be investigated.

The secretion stage of the enamel formation of primary mandibular incisors is to be considered completed at 3-4 months of age. The maturation stage of the enamel formation of primary mandibular incisors is still active at 6 months of age, but is completed at 19 months of age *(*Study *II)*. The enamel formation starts between the 13th and 16th week of gestation of the primary lower incisors (Kraus & Jordan 1965; Lunt & Law 1974). According to this, prenatal formation of enamel is approximately 25 weeks (normal gestation period is 40 weeks) and the postnatal growth is at least 25 weeks (6 months), resulting in a minimum 50 weeks of enamel formation in the primary mandibular incisors. This is in congruence with completion of mineralization of incisors during the first year of life (Levine *et al.* 1979; Lunt & Law 1974).

The initiation of the secretion stage of enamel formation starts at a cusp and the formation proceeds outwards toward the enamel surface and in a cervical direction (Dean 1989; Kraus & Jordan 1965; Rushton 1933). Initiation of enamel development at the most cervical part of the incisor is seen at 1-2 months of age, according to micrographs of tooth buds. The rate of secretion of enamel in the coronal-cervical direction can be estimated to approximately 30 weeks, calculating 25 gestational weeks and around 6 weeks of postnatal growth.

In the microradiographs, the development of tooth formation was seen, both as an enamel and dentin formation and as a root formation. At 19

months of age, the root formation of primary mandibular incisors is still not completed.

5.10 Demineralization *(III)*

Demineralization will change the structure pattern and density in enamel. The loss of minerals affects the orientation of crystals and this influences the appearance in POLMI. In the more porous lesions, the light will diffracted differently. The lesions appeared positively birefringent as a result of being porous. The surface of the lesion was opaque or negatively birefringent, in congruence of earlier investigations (Shellis 1996). The loss of minerals from the interprismatic area will give rise to an appearance of a less mineralized tissue – more radiolucent in the microradiographs.

The gray value, measured by pixels, reflects the density of the minerals in the enamel. Less dense enamel is interpreted as being more porous, resulting in the development of deeper lesions. The relative gray value of the lesion/sound enamel is a measure of a decrease of minerals in each specimen. Assuming sound enamel has different contents of minerals as well as lesions, the relative gray value was calculated in each specimen.

The Ca:P ratio in sound enamel was 2.1, this is in congruence of earlier studies (Robinson *et al.* 1971; Sabel *et al.* 2009). Sound enamel with higher carbon content was shown to have the deepest demineralized lesions. The higher carbon content was interpreted as an enamel with a higher degree of porosity. The reason for this interpretation is the procedure of using cover glass and cyanoacrylate containing glue, in order to keep specimens intact during preparations of thin sections.

Porous enamel was penetrated with cyanoacrylate since the demineralization caused interstitial space in enamel. The cyanoacrylate is easily infiltrated, as seen with other light viscous resins (Meyer-Lueckel & Paris 2008; Robinson *et al.* 2001).

The age depending factor in lesion depth is interpreted as an effect of the oral environment on the posteruptive mineralization. Older individuals have naturally had longer periods of continuous demineralization and remineralization at the enamel surface.

5.11 Factors

The demineralizaton process depends on acid, tooth substance and the frequency and duration of the exposure time in the acid. In order to visualize the dependency of the demineralizing process, a schematic view of a triangle was made (Fig. 36). The acid exposed to the tooth surface is usually from bacteria in the oral biofilm, but may also derive from soft drinks or originate from GERD (Gastroesophageal reflux disease). The tooth substance is either enamel, dentin or root cement, where the individual properties of these tissues must be considered as well. Time is used here as an expression for the duration and frequency of acid exposure.

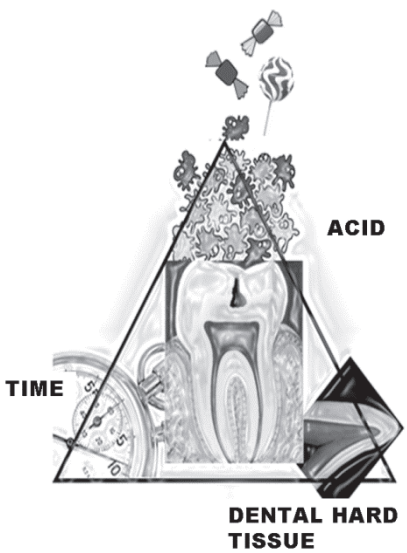

Figure 36. Schematic image of factors of importance for demineralization of dental hard tissues.

5.12 Mind map

In order to visualize parts of the factors affecting the enamel, a mind map was constructed (Fig. 37). The enamel basically undergoes three phases; the secretion stage where the matrix is laid down, the maturation stage where mineralization mainly takes place and the posteruptive phase where constant demineralization and remineralization occurs with important posteruptive maturation due to exposure to the oral environment. The overall picture of enamel is complex. The developing defects in enamel remain in the tissue. The enamel tissue is not rearranged after development is completed. Therefore, morphological and chemical changes in the enamel reveal information regarding the ameloblasts response to conditions in the body during tooth formation.

The enamel of an erupted tooth is constantly being affected in the mouth. The oral biofilm always covers the surface with demineralization and remineralization continuously occuring. The individuality of the enamel and how it affects the affinity of biofilm, etching and bleaching is yet to be investigated.

The secretion stage of ameloblasts is highly vulnerable and defects are likely to occur due to their sensitivity (Massler & Schour 1946; Suga 1989). Hypocalcemia is one factor contributing to hypoplasia (Massler & Schour 1946).

Disturbances during the maturation stage might result in hypomineralized enamel (Suga 1989). The hypomineralized enamel has a lower mechanical resistance in function (Fagrell *et al.* 2010; Fearne *et al.* 2004). Hypomineralized enamel is a more porous enamel and therefore, resistance to caries is likely to be altered. Hypomineralized enamel is clinically seen as white, yellow and/or brown opacities, and the degree of hypomineralization is presumably individual.

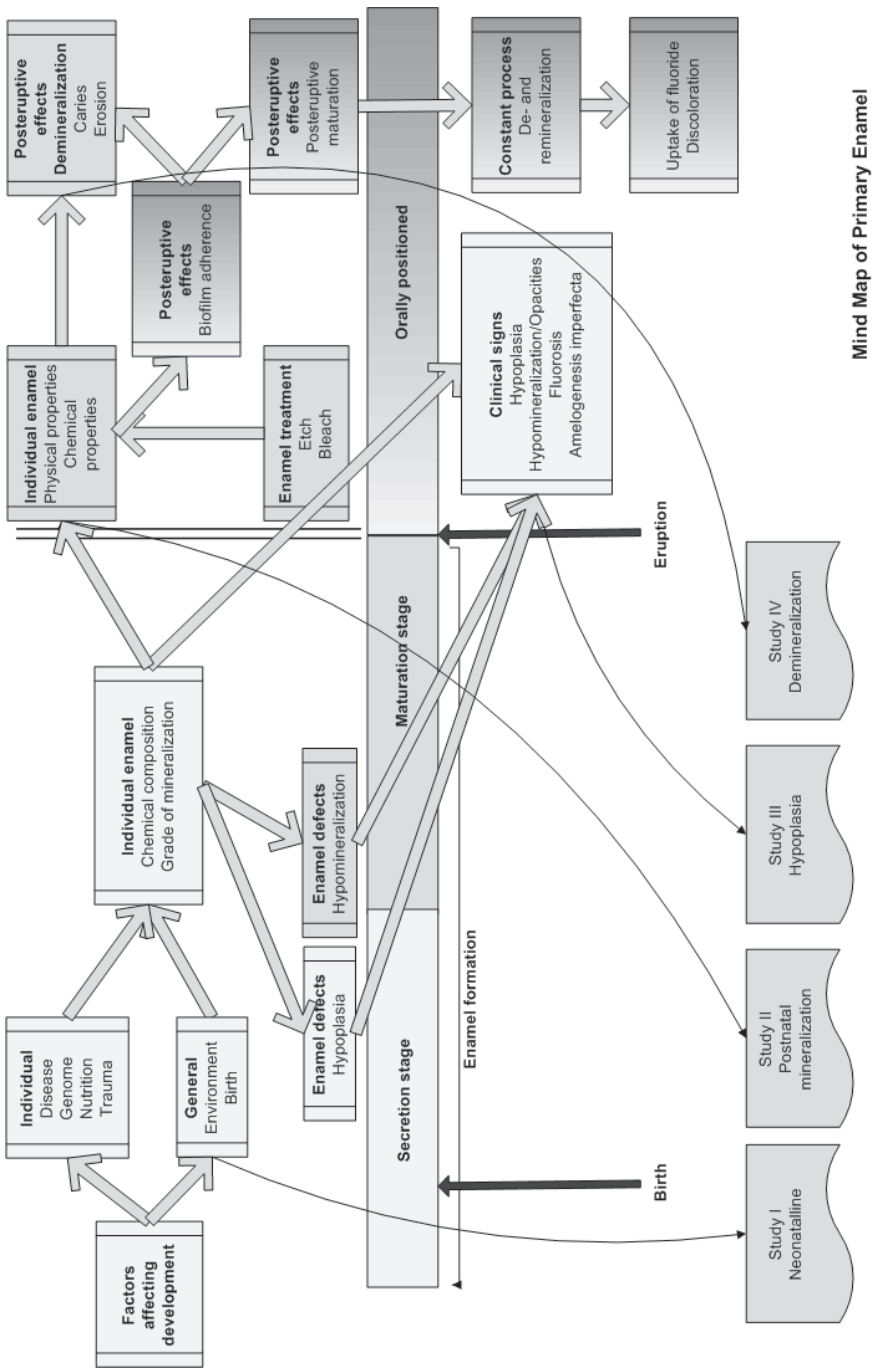

Figure 37. Mind map visualizing factors affecting enamel.

The chemical content of enamel has been seen to differ slightly between individuals (Hallsworth *et al.* 1972; Hallsworth *et al.* 1973; Sabel *et al.* 2009; Wong *et al.* 2004). The response of the individual enamel to demineralization differs. The degree of the porosity of the enamel is affecting the process of demineralization. Additionally, the degree of hypomineralization may alter the process of remineralization. Fluoride is incorporated at the enamel surface as long as the enamel is porous, constituting an available entrance for fluoride (Fejerskov *et al.* 1996). A posteruptive impact of fluoride is found in the enamel as fluoridated hydroxyapatite, formed due to the replacement of some of the hydroxyl groups in the hydroxyapatite, or as a calcium fluoride formed on the enamel apatite crystal surface (Fejerskov *et al.* 1996). The fluoridated hydroxyapatite is more resistant to demineralization compared to hydroxyapatite (Fejerskov *et al.* 1996).

The morphological and chemical aspects of the neonatal line are described in Study *I*. Postnatal mineralization is discussed in Study *II*. The enamel developmental defect, hypoplasia, is histologically described in Study *III*. Description of the chemical content and degree of mineralization related to demineralization, is investigated in Study *IV*.

6 CONCLUSIONS

- The neonatal line is a hypomineralized structure with a rupture in the enamel matrix due to disturbances during the enamel secretion stage. The enamel prisms postnatally appear to be smaller than the prenatal prisms. There is no alteration in the chemical composition in the prenatal compared with the postnatal enamel.
- Postnatal enamel mineralizes with a gradient maturation; the maturation is still continuous at 6 months of age.
- The buccal enamel of primary mandibular incisors has reached its full thickness (~380 μm) by 3-4 months of age.
- Enamel hypoplasia is an enamel developmental defect with rounded cervical borders. The rounded border is an effect of bent prisms of normal length. The enamel of the rounded border appeared partly hypomineralized, due to the bent prisms not being as densely packed as prisms are in normal enamel.
- The base of the hypoplasia has a rough surface and no aprismatic surface layer is found.
- Demineralization of enamel is dependent on the mineral and chemical content of the enamel exposed. More porous enamel develops deeper lesions.
- The posteruptive maturation of enamel is of importance for the resistance to demineralization, where children older than 8.2 years showed the most shallow lesions.

7 CLINICAL IMPLICATIONS

- Hypomineralization at the bottom of an enamel hypoplasia may be more predisposed to caries.
- The chemical content and degree of mineralization of primary enamel differed between different teeth/individuals. In a more porous enamel, deeper lesions develop in a shorter period of time.
- The degree of mineralization of enamel is not possible to verify clinically. Therefore, the posteruptive maturation of enamel is important for resistance to demineralization, which may be optimized by local fluoride treatment.

ACKNOWLEDGEMENTS

First and foremost, I would like to thank everyone who has been helping me during these years and who have given me encouraging words and positive feedback.

I especially wish to thank:

Professor Jörgen G. Norén, my supervisor, for introducing me to the world of science and research, and for his fantastic encouragement and patience with me, for all the help and interest he has shown in my work and for letting me be part of his work.

Associate Professor Agneta Robertson, my co-supervisor, for believing in me and for always responding in a constructive way.

Sandra Ståhlberg, for excellent proofreading.

Wolfram Dietz, Frank Steiniger, Sandor Nietzsche, and the rest of the team at Centre of Electron Microscopy, Friedrich-Schiller-University, Jena, Germany, for being helpful with the work at the microscope and collaboration.

The patients who donated their teeth for research and their parents for allowing participation in the study.

My dear parents, Ulla and Ingvar, who have always encouraged me.

Finally and most importantly, my wonderful family. Robert, my beloved husband, and our two children Clara and Carl:

You are the sunshine of my life!

The studies have been supported by grants from: The Gothenburg Dental Society, Gothenburg, Sweden; FOU, Public Dental Care, Region Västra Götaland, Sweden; Swedish Society of Pediatric Dentistry; Martina & Wilhelm Lundgrens Vetenskapsfond II.

REFERENCES

18th WMA General Assembly, H., Finland, June 1964. (2008). "http://www.wma.net/en/30publications/10policies/b3/17c.pdf." Retrieved 2011-11-08, 2011.

Abramowitz, M. & Davidson, W. M. (2010). "Optical Birefringence." http://www.olympusmicro.com/primer/lightandcolor/birefringence.html Retrieved 2011-11-23, 2011.

Aguirre, J. M., Rodriguez, R., Oribe, D. & Vitoria, J. C. (1997). Dental enamel defects in celiac patients. *Oral Surg Oral Med Oral Pathol Oral Radiol Endod,* 84, 646-650.

Aine, L., Maki, M., Collin, P. & Keyrilainen, O. (1990). Dental enamel defects in celiac disease. *J Oral Pathol Med,* 19, 241-245.

Allan, J. H. (1959). Investigations into the mineralization pattern of human dental enamel. *J Dent Res,* 38, 1096-1128.

Boyde, A. (1997). Microstructure of enamel. *Ciba Found Symp,* 205, 18-27; discussion 27-31.

Clarkson, J. (1989). Review of terminology, classifications, and indices of developmental defects of enamel. *Adv Dent Res,* 3, 104-109.

Dawes, C. & Jenkins, G. N. (1962). Some inorganic constituents of dental plaque and their relationship to early calculus formation and caries. *Arch Oral Biol,* 7, 161-172.

Dean, M. C. (1989). The developing dentition and tooth structure in hominoids. *Folia Primatol (Basel),* 53, 160-176.

den Besten, P. K. (1986). Effects of fluoride on protein secretion and removal during enamel development in the rat. *J Dent Res,* 65, 1272-1277.

Derise, N. L. & Ritchey, S. J. (1974). Mineral composition of normal human enamel and dentin and the relation of composition to dental caries. II. Microminerals. *J Dent Res,* 53, 853-858.

Deutsch, D., Palmon, A., Dafni, L., Mao, Z., Leytin, V., Young, M. & Fisher, L. W. (1998). Tuftelin--aspects of protein and gene structure. *Eur J Oral Sci,* 106 Suppl 1, 315-323.

Ehrlich, H., Koutsoukos, P. G., Demadis, K. D. & Pokrovsky, O. S. (2008). Principles of demineralization: modern strategies for the isolation of organic frameworks. Part I. Common definitions and history. *Micron,* 39, 1062-1091.

Ehrlich, H., Koutsoukos, P. G., Demadis, K. D. & Pokrovsky, O. S. (2009). Principles of demineralization: modern strategies for the isolation of organic frameworks. Part II. Decalcification. *Micron,* 40, 169-193.

Fagrell, T. G., Dietz, W., Jalevik, B. & Norén, J. G. (2010). Chemical, mechanical and morphological properties of hypomineralized enamel of permanent first molars. *Acta Odontol Scand,* 68, 215-222.

Fearne, J., Anderson, P. & Davis, G. R. (2004). 3D X-ray microscopic study of the extent of variations in enamel density in first permanent molars with idiopathic enamel hypomineralisation. *Br Dent J,* 196, 634-638; discussion 625.

Fearne, J. M., Elliott, J. C., Wong, F. S., Davis, G. R., Boyde, A. & Jones, S. J. (1994). Deciduous enamel defects in low-birth-weight children: correlated X-ray microtomographic and backscattered electron imaging study of hypoplasia and hypomineralization. *Anat Embryol (Berl),* 189, 375-381.

Fejerskov, O., Silverstone, L. M., Melsen, B. & Moller, I. J. (1975). Histological features of fluorosed human dental enamel. *Caries Res,* 9, 190-210.

Fejerskov, O., Baelum, V., Manji, F. & Möller, I. (1988). *Dental fluorosis - a handbook for health workers*. Copenhagen, Munksgaard.

Fejerskov, O., Ekstrand, J. & Burt, B. A. (1996). *Fluoride in dentistry*. Copenhagen, Minksgaard.

Forslind, B. (1981). *Elektronmikroskopi - teori och praktik*. Stockholm, Almqvist och Wiksell Förlag AB.

Garnett, J. & Dieppe, P. (1990). The effects of serum and human albumin on calcium hydroxyapatite crystal growth. *Biochem J,* 266, 863-868.

Gustafson, A. G. (1959). A morphological investigation of certain variations in the structure and mineralization of human dental enamel. *Odontologisk Tidsskrift,* 365-466.

Hallsworth, A. S., Robinson, C. & Weatherbell, J. A. (1972). Mineral and magnesium distribution within the approximal carious lesion of dental enamel. *Caries Res,* 6, 156-168.

Hallsworth, A. S., Weatherell, J. A. & Robinson, C. (1973). Loss of carbonate during the first stages of enamel caries. *Caries Res,* 7, 345-348.

Helmcke, J.-G., Schulz, L. & Scott, D. B. (1963). Querstreifung der menschlichen Schmelzprismen. *Deutsche Zahnärztl. Z,* 18, 569-575, 626-637.

Hong, L., Levy, S. M., Warren, J. J. & Broffitt, B. (2009). Association between enamel hypoplasia and dental caries in primary second molars: a cohort study. *Caries Res,* 43, 345-353.

Hu, J. C., Chun, Y. H., Al Hazzazzi, T. & Simmer, J. P. (2007). Enamel formation and amelogenesis imperfecta. *Cells Tissues Organs,* 186, 78-85.

Hu, J. C., Hu, Y., Smith, C. E., McKee, M. D., Wright, J. T., Yamakoshi, Y., Papagerakis, P., Hunter, G. K., Feng, J. Q., Yamakoshi, F. & Simmer, J. P. (2008). Enamel defects and ameloblast-specific expression in Enam knock-out/lacz knock-in mice. *J Biol Chem,* 283, 10858-10871.

Kraus, B. S. & Jordan, R. E. (1965). *The human dentition before birth*. Philadelphia, Lea & Febiger.

Kraus, B. S. & Jordan, R. E. (1965). *The human dentition before birth*. Philadelphia, Lea & Febiger.

Lakomaa, E. L. & Rytomaa, I. (1977). Mineral composition of enamel and dentin of primary and permanent teeth in Finland. *Scand J Dent Res,* 85, 89-95.

Levine, R. S., Turner, E. P. & Dobbing, J. (1979). Deciduous teeth contain histories of developmental disturbances. *Early Hum Dev.,* 3, 211-220.

Lodding, A. (1997). SIMS of biomineralized tissues: present trends and potentials. *Adv Dent Res,* 11, 364-379.

Lodding, A., Frostell, G., Kkoch, G., Norén, J., Odelius, H., Petersson, LG (1981). Ion probe and electron probe study of element concentrations at different depths in sound and hypomineralized teeth. *J Microsc Spectrosc electron,* 6, 201-211.

Lunt, R. C. & Law, D. B. (1974). A review of the chronology of calcification of deciduous teeth. *J Am Dent Assoc.,* 89, 599-606.

Margolis, H. C. & Moreno, E. C. (1992). Kinetics of hydroxyapatite dissolution in acetic, lactic, and phosphoric acid solutions. *Calcif Tissue Int,* 50, 137-143.

Massler, M. & Schour, I. (1946). Growth of the child and the calcification pattern of the teeth. *Am J Orthod Oral Surg,* 32, 495-517.

Meyer-Lueckel, H. & Paris, S. (2008). Improved resin infiltration of natural caries lesions. *J Dent Res,* 87, 1112-1116.

Morad, D. & Ryr, C. (2010). Manual för mikroskopering - undervisningsmaterial för grundutbildning.

Needleman, H. L., Leviton, A. & Allred, E. (1991). Macroscopic enamel defects of primary anterior teeth--types, prevalence, and distribution. *Pediatr Dent,* 13, 208-216.

Nikiforuk, G. & Fraser, D. (1981). The etiology of enamel hypoplasia: a unifying concept. *J Pediatr,* 98, 888-893.

Norén, J. G., Grahnen, H. & Magnusson, B. O. (1978). Maternal diabetes and changes in the hard tissues of primary teeth. III. A histologic and microradiographic study. *Acta Odontol Scand.,* 36, 127-135.

Norén, J. G. (1983). Enamel structure in deciduous teeth from low-birth-weight infants. *Acta Odontol Scand,* 41, 355-362.

Norén, J. G., Lodding, A., Odelius, H. & Linde, A. (1983). Secondary ion mass spectrometry of human deciduous enamel. Distribution of Na, K, Mg, Sr, F and Cl. *Caries Res,* 17, 496-502.

Norén, J. G. (1984). Microscopic study of enamel defects in deciduous teeth of infants of diabetic mothers. *Acta Odontol Scand.,* 42, 153-156.

Norén, J. G. & Engstrom, C. (1987). Cutting mineralized hard tissues with the Leitz low-speed saw microtome. *Leitz Mitt. Tech.,* 49-52.

Oliveira, A. F., Chaves, A. M. & Rosenblatt, A. (2006). The influence of enamel defects on the development of early childhood caries in a population with low socioeconomic status: a longitudinal study. *Caries Res,* 40, 296-302.

Radlanski, R. J. & Renz, H. (2006). Developmental movements of the inner enamel epithelium as derived from micromorphological features. *Eur J Oral Sci.,* 114, 343-348; discussion 349-350, 382.

Ranggard, L. & Norén, J. G. (1994). Effect of hypocalcemic state on enamel formation in rat maxillary incisors. *Scand J Dent Res,* 102, 249-253.

Ranggard, L., Norén, J. G. & Nelson, N. (1994). Clinical and histologic appearance in enamel of primary teeth in relation to neonatal blood ionized calcium values. *Scand J Dent Res,* 102, 254-259.

Ranggard, L., Ostlund, J., Nelson, N. & Norén, J. G. (1995). Clinical and histologic appearance in enamel of primary teeth from children with neonatal hypocalcemia induced by blood exchange transfusion. *Acta Odontol Scand,* 53, 123-128.

Risnes, S. (1990). Structural characteristics of staircase-type Retzius lines in human dental enamel analyzed by scanning electron microscopy. *Anat Rec,* 226, 135-146.

Robinson, C., Weatherell, J. A. & Hallsworth, A. S. (1971). Variatoon in composition of dental enamel within thin ground tooth sections. *Caries Res,* 5, 44-57.

Robinson, C., Briggs, H. D. & Atkinson, P. J. (1981). Histology of enamel organ and chemical composition of adjacent enamel in rat incisors. *Calcif Tissue Int,* 33, 513-520.

Robinson, C., Kirkham, J., Stonehouse, N. J. & Shore, R. C. (1989). Control of crystal growth during enamel maturation. *Connect Tissue Res,* 22, 139-145.

Robinson, C., Kirkham, J., Brookes, S. J. & Shore, R. C. (1992). The role of albumin in developing rodent dental enamel: a possible explanation for white spot hypoplasia. *J Dent Res,* 71, 1270-1274.

Robinson, C., Brookes, S. J., Shore, R. C. & Kirkham, J. (1998). The developing enamel matrix: nature and function. *Eur J Oral Sci,* 106 Suppl 1, 282-291.

Robinson, C., Brookes, S. J., Kirkham, J., Wood, S. R. & Shore, R. C. (2001). In vitro studies of the penetration of adhesive resins into artificial caries-like lesions. *Caries Res,* 35, 136-141.

Rozier, R. G. & Dudney, G. G. (1981). Dental fluorosis in children exposed to multiple sources of fluoride: implications for school fluoridation programs. *Public Health Rep,* 96, 542-546.

Rushton, M. (1933). On the fine contour lines of the enamel of milk teeth. *The dental record,* 53, 170-171.

Rythén, M., Sabel, N., Dietz, W., Robertson, A. & Norén, J. G. (2010). Chemical aspects on dental hard tissues in primary teeth from preterm infants. *Eur J Oral Sci,* 118, 389-395.

Sabel, N., Dietz, W., Lundgren, T., Nietzsche, S., Odelius, H., Rythén, M., Rizell, S., Robertson, A., Norén, J. G. & Klingberg, G. (2009). Elemental composition of normal primary tooth enamel analyzed with XRMA and SIMS. *Swed Dent J,* 33, 75-83.

Sasaki, T., Takagi, M. & Yanagisawa, T. (1997). Structure and function of secretory ameloblasts in enamel formation. *Ciba Found Symp,* 205, 32-46; discussion 46-50.

Schour, I. (1936). The neonatal line in enamel and dentin of the human deciduous teeth and first permanent molar. *Jour. A.D.A.,* 23, 1946-1955.

Shellis, R. P. (1996). A scanning electron-microscopic study of solubility variations in human enamel and dentine. *Arch Oral Biol,* 41, 473-484.

Simmer, J. P., Hu, Y., Lertlam, R., Yamakoshi, Y. & Hu, J. C. (2009). Hypomaturation enamel defects in Klk4 knockout/LacZ knockin mice. *J Biol Chem,* 284, 19110-19121.

Skobe, Z. (2006). SEM evidence that one ameloblast secretes one keyhole-shaped enamel rod in monkey teeth. *Eur J Oral Sci.,* 114, 338-342; discussion 349-350, 382.

Suga, S. (1989). Enamel hypomineralization viewed from the pattern of progressive mineralization of human and monkey developing enamel. *Adv Dent Res,* 3, 188-198.

Szpringer-Nodzak, M. (1984). The location of the neonatal line in human enamel. *J Int Assoc Dent Child,* 15, 1-6.

Taji, S. S., Seow, W. K., Townsend, G. C. & Holcombe, T. (2011). Enamel hypoplasia in the primary dentition of monozygotic and dizygotic twins compared with singleton controls. *Int J Paediatr Dent,* 21, 175-184.

Teivens, A., Mornstad, H., Norén, J. G. & Gidlund, E. (1996). Enamel incremental lines as recorders for disease in infancy and their relation to the diagnosis of SIDS. *Forensic Sci Int.,* 81, 175-183.

Ten Cate, A. R. (1994). *Oral Histology: development, structure, and function*. St Louis, Mosby.

ten Cate, J. M., Dundon, K. A., Vernon, P. G., Damato, F. A., Huntington, E., Exterkate, R. A., Wefel, J. S., Jordan, T., Stephen, K. W. & Roberts, A. J. (1996). Preparation and measurement of artificial enamel lesions, a four-laboratory ring test. *Caries Res,* 30, 400-407.

Termine, J. D., Belcourt, A. B., Christner, P. J., Conn, K. M. & Nylen, M. U. (1980). Properties of dissociatively extracted fetal tooth matrix proteins. I. Principal molecular species in developing bovine enamel. *J Biol Chem,* 255, 9760-9768.

Thylstrup, A. & Fejerskov, O. (1986). *Textbook of cariology.* . Copenhagen, Munksgaard.

Thylstrup, A. & Fejerskov, O. (1994). *Textbook of clinical cariology*. Copenhagen, Munksgaard.

Vello, M. A., Martinez-Costa, C., Catala, M., Fons, J., Brines, J. & Guijarro-Martinez, R. (2010). Prenatal and neonatal risk factors for the development of enamel defects in low birth weight children. *Oral Dis,* 16, 257-262.

Vieira, A. P., Hanocock, R., Eggertsson, H., Everett, E. T. & Grynpas, M. D. (2005). Tooth quality in dental fluorosis genetic and environmental factors. *Calcif Tissue Int,* 76, 17-25.

Whittaker, D. K. (1982). Structural variations in the surface zone of human tooth enamel observed by scanning electron microscopy. *Arch Oral Biol,* 27, 383-392.

Wong, F. S., Anderson, P., Fan, H. & Davis, G. R. (2004). X-ray microtomographic study of mineral concentration distribution in deciduous enamel. *Arch Oral Biol,* 49, 937-944.

Wright, J. T., Hall, K. & Yamauchi, M. (1997). The protein composition of normal and developmentally defective enamel. *Ciba Found Symp,* 205, 85-99; discussion 99-106.

Yoshioka, M., Yoshida, Y., Inoue, S., Lambrechts, P., Vanherle, G., Nomura, Y., Okazaki, M., Shintani, H. & Van Meerbeek, B. (2002). Adhesion/decalcification mechanisms of acid interactions with human hard tissues. *J Biomed Mater Res,* 59, 56-62.

Zhang, Y., Yan, Q., Li, W. & DenBesten, P. K. (2006). Fluoride down-regulates the expression of matrix metalloproteinase-20 in human fetal tooth ameloblast-lineage cells in vitro. *Eur J Oral Sci,* 114 Suppl 1, 105-110; discussion 127-109, 380.